# **Manuscript Details**

Manuscript number MARGO\_2017\_112

Title Baffin Bay Paleoenviroments in the LGM and HS1: Resolving the ice-shelf

question

Article type Research Paper

#### **Abstract**

Core HU2008029-12PC from the Disko trough mouth fan on the central West Greenland continental slope is used to test whether an ice shelf covered Baffin Bay during the Last Glacial Maximum (LGM) and at the onset of the deglaciation. We use benthic and planktic foraminiferal assemblages, stable isotope analysis of planktic forams, algal biomarkers, ice-rafted detritus (IRD), lithofacies characteristics defined from CT scans, and quantitative mineralogy to reconstruct paleoceanographic conditions, sediment processes and sediment provenance. The chronology is based on radiocarbon dates on planktic foraminifers using a ΔR of 140 ± 30 14C years, supplemented by the varying reservoir estimates of Stern and Lisiecki (2013) that provide an envelope of potential ages. HU2008029-12PC is bioturbated throughout. Sediments between the core base at 11.3 m and 4.6 m (LGM through HS1) comprise thin turbidites, plumites and hemipelagic sediments with Greenlandic provenance consistent with processes active at the Greenland Ice Sheet margin grounded at or near the shelf edge. Abundance spikes of planktic forams coincide with elevated abundance of benthic forams in assemblages indicative of chilled Atlantic Water, meltwater and intermittent marine productivity. IRD and IP25 are rare in this interval, but brassicasterol, an indicator of marine productivity reaches and sustains low levels during the LGM. These biological characteristics are consistent with a sea-ice covered ocean experiencing periods of more open water such as leads or polynyas in the sea ice cover, with chilled Atlantic Water at depth, rather than full ice-shelf cover. There is no supporting data for the existence of a full Baffin Bay ice shelf cover extending from grounded ice on the Davis Strait. Initial Greenland Ice Sheet retreat from the West Greenland margin is manifested by a pronounced lithofacies shift to bioturbated, diatomaceous mud with rare IRD of Greenlandic origin at 467 cm (16.2 cal ka BP; ΔR=140 yrs) within Heinrich Stadial 1 (HS1). A spike in foraminiferal abundance and ocean warmth indicator benthic forams precedes the initial ice retreat from the shelf edge. At the end of HS1, IP25, brassicasterol and benthic forams indicative of sea-ice edge productivity increase, indicating warming interstadial conditions. Within the Bølling/Allerød interstadial a strong rise in IP25 content and IRD spikes rich in detrital carbonate from northern Baffin Bay indicate that northern Baffin Bay ice streams were retreating and provides evidence for increased open water, advection of Atlantic Water in the West Greenland Current, and formation of an IRD belt along the W. Greenland margin.

**Keywords** Arctic ocean and adjacent high latitudes; micropaleontology (forams);

paleooceanography; Glacial sediments

**Taxonomy** Ice Sheets, Paleoceanography, Quaternary Stratigraphy

Corresponding Author Anne Jennings

Order of Authors Anne Jennings, John Andrews, Colm O'Cofaigh, Guillaume St-Onge, Simon

Belt, Patricia Cabedo Sanz, Christof Pearce, Claude Hillaire-Marcel, Calvin

Campbell

Suggested reviewers Leonid Polyak, Svend Funder, Richard Alley, Paul Knutz, Quentin Simon, Karen

Luise Knudsen, Lev Tarasov

### **Submission Files Included in this PDF**

# File Name [File Type]

Margo\_revision\_letter\_Jennings\_8\_15\_17.doc [Response to Reviewers]

12PC LGM paper\_8\_4\_2017\_revision.docx [Revised Manuscript with Changes Marked]

Highlights.docx [Highlights]

12PC\_MARGO\_cleanrvised\_8\_14\_2017.docx [Manuscript File]

Fig.1\_MG\_rev.jpg [Figure]

Anne\_jennings\_figure2\_revised.jpg [Figure]

Fig\_3\_12PCrev\_mar\_geol.jpg [Figure]

Fig\_4.jpg [Figure]

Fig 5.jpg [Figure]

Fig\_6rev\_12PC\_benthics\_MGpaper.jpg [Figure]

Fig\_7.jpg [Figure]

Table 1\_MG.xlsx [Table]

To view all the submission files, including those not included in the PDF, click on the manuscript title on your EVISE Homepage, then click 'Download zip file'.

### Research Data Related to this Submission

### Data set

https://data.mendeley.com/datasets/5c67tv7c74/draft?a=176055ec-dbe3-426c-a58d-05b30e1fe70a

Data for: Baffin Bay Paleoenviroments in the LGM and HS1: Resolving the ice-shelf question

These data are for publication in Marine Geology for the special issue on Glaciated Continental Margins

# Baffin Bay Paleoenvironments in the LGM and HS1: Resolving the ice-shelf question

4 Anne E. Jennings<sup>1\*</sup>, John T. Andrews<sup>1</sup>, Colm Ó Cofaigh<sup>2</sup>, Guillaume St-Onge<sup>3</sup>, Simon

- 5 Belt<sup>4</sup>, Patricia Cabedo-Sanz<sup>4</sup>, Christof Pearce<sup>5</sup>, Claude Hillaire-Marcel<sup>7</sup>, D. Calvin
- 6 Campbell<sup>8</sup>

1

2

3

22

23 24

25

26

27

28

29

30 31

32

33

34

35

36 37

38

39

40

41

42

43

44 45

46

47

48 49

50

- 7 INSTAAR University of Colorado, Campus Box 450, Boulder, CO 80309-0450 USA
- <sup>2</sup> Department of Geography, Durham University, South Road, Durham DH1 3LE, United
   Kingdom
- <sup>3</sup> Institut des sciences de la mer de Rimouski (ISMER) Université du Québec à Rimouski
   11 and GEOTOP Rimouski, Québec, Canada S5L 3A1
- School of Geography, Earth and Environmental Sciences, University of Plymouth,
   Plymouth PL4 8AA United Kingdom
- Department of Geological Sciences and Bolin Centre for Climate Research, Stockholm
   University, Svante Arrhenius väg 8, SE-106 91 Stockholm, Sweden
- 16 <u>6 Department of Geoscience and Arctic Research Centre, Aarhus University, Hoegh</u>
- 17 <u>Guldbergs gade 2, 8000 Aarhus, Denmark</u>
- 18 <sup>1</sup> Université du Québec a Montréal, Centre GEOTOP CP 8888, succ. Centre-Ville,
- 19 Montréal, Québec, Canada, H3C 3P8
- Egeological Survey of Canada-Atlantic, Natural Resources Canada, Dartmouth Nova
   Scotia
  - \* anne.jennings@colorado.edu

Core HU2008029-12PC from the Disko trough mouth fan on the central West Greenland continental slope is used to test whether an ice shelf covered Baffin Bay during the Last Glacial Maximum (LGM) and at the onset of the deglaciation. We use benthic and planktic foraminiferal assemblages, stable isotope analysis of planktic forams, algal biomarkers, ice-rafted detritus (IRD), lithofacies characteristics scans, and quantitative mineralogy to from CT paleoceanographic conditions, sediment processes and sediment provenance. The chronology is based on radiocarbon dates on planktic foraminifers using a  $\Delta R$  of 140 ± 30 <sup>14</sup>C years, supplemented by the varying reservoir estimates of Stern and Lisiecki (2013) that provide an envelope of potential ages. HU2008029-12PC is bioturbated throughout. Sediments between the core base at 11.3 m and 4.6 m (LGM through HS1) comprise thin turbidites, plumites and hemipelagic sediments with Greenlandic provenance consistent with processes active at the Greenland Ice Sheet margin grounded at or near the shelf edge. Abundance spikes of planktic forams coincide with elevated abundance of benthic forams in assemblages indicative of chilled Atlantic Water, meltwater and intermittent marine productivity. IRD and IP<sub>25</sub> are rare in this interval, but brassicasterol, an indicator of marine productivity reaches and sustains low levels during the LGM. These biological characteristics are consistent with a sea-ice covered ocean experiencing periods of more open water such as leads or polynyas in the sea ice cover, with chilled Atlantic Water at depth, rather than full ice-shelf cover. They do not support the existence of a full Baffin Bay ice shelf cover extending from grounded ice on the Davis Strait. Initial ice retreat from the West Greenland margin is manifested by a pronounced lithofacies shift to bioturbated, diatomaceous mud with rare IRD of Greenlandic origin at 467 cm (16.2 cal ka BP;  $\Delta R$ =140 yrs) within HS1. A spike in foraminiferal abundance and ocean warmth indicator benthic forams precedes the initial ice retreat from the shelf edge. At the end of HS1, IP<sub>25</sub>, brassicasterol and benthic

forams indicative of sea-ice edge productivity increase, indicating warming interstadial conditions. Within the Bølling/Allerød interstadial a strong rise in IP<sub>25</sub> content and IRD spikes rich in detrital carbonate from northern Baffin Bay indicate that northern Baffin Bay ice streams were retreating and provides evidence for increased open water, advection of Atlantic Water in the West Greenland Current, and formation of an IRD belt along the W. Greenland margin.

57 58

Keywords: Greenland Ice Sheet, Baffin Bay, paleoceanography, ice shelf, foraminifera, Heinrich Stadial 1

59 60

### 1. Introduction

62

63

64

65

66

67

68

69

70

71

72

73

74

75

76

77

78

61

Last Glacial Maximum (LGM) climatic and oceanic conditions in Baffin Bay are currently poorly known, but according to the temperature reconstructions from the Greenland Ice Sheet borehole (Dahl-Jensen and al., 1998) and ice-core data (Buizert et al., 2014), summit temperatures were ~20°C colder than present. Applying this temperature difference down to sea level using the adiabatic lapse rate, suggests that the annual temperature at the surface of Baffin Bay adjacent to Baffin Island would approach -36°C. Such cold temperatures support the argument that cold-based ice covered the forelands of eastern Baffin Island (Briner et al., 2003) with "Antarctic-like" conditions across Baffin Bay, which would also suggest that Baffin Bay was covered in perennial sea ice. At the LGM, confluent, Innuitian (IIS), Laurentide (LIS) and Greenland (GIS) ice sheets (England et al., 2006) blocked the channels that connect Baffin Bay to the Arctic Ocean (Dyke, 2002) and terminated in northern Baffin Bay as large ice streams (Li et al., 2011; Blake, 1977). The Greenland ice sheet reached the continental shelf edge via large ice streams off west Greenland (Ó Cofaigh et al., 2013a; Jennings et al., in revision 2017; Slabon et al., 2016; Sheldon et al., 2016; Dowdeswell et al., 2014), but the outer limits of the ice on the Baffin shelf are not known.

On the basis of modeling, it has been proposed that Baffin Bay was blocked at its
southern end by an ice shelf extension of the Hudson Strait ice stream that grounded
across Davis Strait to reach southern Greenland, thus sealing Baffin Bay from the
Labrador Sea (Hulbe et al., 1997; Álvarez-Solas et al., 2010; Marcott et al., 2011). This
ice shelf was the starting point for modeling the processes that produce Heinrich events
(Hulbe et al., 1997; Álvarez-Solas et al., 2010; Marcott et al., 2011), but physical
evidence for it has not been recovered. An ice shelf of this scale would have
environmental consequences that should be recorded in Baffin Bay sediments. Firstly,
grounding of a Labrador Sea ice shelf along Davis Strait would prevent seawater
exchange between Baffin Bay and the Labrador Sea, excluding advection of organic
matter into Baffin Bay. It also would shut down in situ primary marine productivity in
Baffin Bay so that planktic and benthic organisms, their biomarkers, and bioturbation
would be absent in the sediment. Secondly, ice shelves and even extensive sea-ice cover
are known to restrict the movement and export of icebergs (Reeh et al., 2001; Domack
and Harris, 1998). Thus iceberg rafting and mixing of sediments of various provenances
in Baffin Bay would be reduced. Using these concepts, we test the LGM Baffin Bay ice-
shelf hypothesis by studying the sedimentological and biological characteristics of
sediments in HU2008029-12PC from the continental slope off western Greenland, a core
that extends from the LGM into the Younger Dryas (YD) and that recorded retreat of the
Greenland Ice Sheet during deglaciation (Jennings et al., in revision 2017).

# 2. Setting of core HU2008029-12PC

Detailed studies of LGM and deglacial environments in Baffin Bay have been hampered by relatively slow sediment accumulation rates and poor calcium carbonate preservation (cf. Aksu, 1985; de Vernal et al., 1992; Simon et al., 2012). HU2008029-12PC (hereafter called 12PC) was raised from the northern side of the Disko trough mouth fan (TMF) from acoustically stratified sediments with continuous parallel reflections on the eastern side of Baffin Bay (68°13.69' N; 57°37.08' W; 1475 m water depth; Campbell and de Vernal, 2009) (Figs. 1 and 2). This site on the trough mouth fan has higher sediment accumulation than sites in the deep basin of Baffin Bay that have variable sedimentation rates that range between 3 and 35 cm/ka (Andrews et al., 1998; Hillaire-Marcel et al., 1989, 2004; Simon et al., 2012; 2014) (Fig. 1). The Disko TMF was built throughout the Quaternary by rapid sediment deposition in front of the fast flowing Disko ice stream (Fig. 1) when the GIS margin was

deposition in front of the fast flowing Disko ice stream (Fig. 1) when the GIS margin was extended on the shelf, and from hemipelagic sedimentation during and after ice retreat (ÓCofaigh et al., 2013a, b; Jennings et al., in revision2017; Hofmann et al., 2016). An ice sheet grounded at or near the shelf edge delivers abundant sediments directly to the continental slope in the form of sediment gravity flows, including turbidity currents that form graded sand layers, stratified sand/silt beds, and glacigenic debris flows (ÓCofaigh et al., 2013a, b, Lucci and Rebesco, 2007). Turbid meltwater plumes released from the ice front produce plumites, which are finer grained than the turbidites as the sand is dropped near the ice front and the silt and clay continue offshore in suspension (Hesse et al., 1997; Lucchi and Rebesco, 2007). Depending on sea surface conditions such as perennial sea ice and/or ice shelves, icebergs would also deliver sediment to the slope as

they melted during their transit in Baffin Bay (Andrews et al., 1998; 2014; Jennings et al., 2014; Simon et al., 2012; 2014; 2016; Sheldon et al., 2016).

Each year, the The modern sea ice edge extends southeast to northwest within

Baffin Bay and sea ice cover is greater in the western than in the eastern half due to the

Baffin Bay and sea ice cover is greater in the western than in the eastern half due to the influence of the relatively warm and saline West Greenland Current that enters Baffin Bay from the southeast (Tang et al., 2004; Münchow et al., 2015) (Fig. 1). The boundary between lower salinity, sea-ice bearing, Arctic Surface Water (ASW) that passes from the Arctic Ocean through the channels of the Canadian Arctic Archipelago into Baffin Bay and Atlantic Waters of the West Greenland Current (WGC) moving northward along West Greenland is oriented NE-SW and migrates through the year. The relatively warm, saline Atlantic Water submerges beneath the ASW (Buch, 2000a, b) and forms the West Greenland Intermediate Water (WGIW) (Fig. 1 inset) (Tang et al., 2004). During the LGM, however, the circulation regime in Baffin Bay would have been different because the southward flow of ASW into Baffin Bay was blocked by confluent ice sheets grounded in the channels of the Canadian Arctic Archipelago until the early Holocene (England, 1999; Zreda et al., 1999; Jennings et al., 2011a; Piénkowski et al., 2011). Today, warm Atlantic Water carried in the WGC accesses the GIS margins via cross shelf troughs and fjords, where the ice sheet terminates in the sea (Holland et al., 2008) and promotes basal melting (Straneo et al., 2012). WGC Atlantic Water flow was initiated as early as 14.4 cal ka BP off central West Greenland and is implicated in Greenland Ice Sheet retreat from the LGM position at the shelf edge (cf. Knutz et al., 2011; Sheldon et al., 2016; Jennings et al., in revision 2017).

145

123

124

125

126

127

128

129

130

131

132

133

134

135

136

137

138

139

140

141

142

143

### 3. Methods:

146

147 3.1 Age Model 148 The age model for 12PC is based on 7 radiocarbon dates between 201 and 860 cm on the 149 arctic planktic foraminifer, Neogloboquadrina pachyderma (sensu Darling et al., 2006). 150 The dates were previously published in Jennings et al., (in revision 2017) (Table 1). 151 Radiocarbon dates were calibrated using the Marine 13 curve (Reimer et al., 2013). OxCal 152 version 4.2.4 (Ramsey and Lee, 2013) was used to compute an age/depth model (Fig. 3). 153 An age reversal in the upper 110 cm of the core limited the chronology to the interval 154 from 200 cm to the base of the core (1130 cm). The age of the core base is assumed to be 155 no older than 26.5 ka BP, the beginning of the LGM (Clark et al., 2009). This assumed 156 basal age results in a large uncertainty in the modeled age of the base of the core (24 to 157 28 cal ka BP). Given this basal age, we might expect to record Baffin Bay Detrital 158 Carbonate (BBDC) event BBDC3 that is found in central Baffin Bay from c. 23.5 to 25 159 cal ka BP (Simon et al., 2016). A single data point with 20% NBB source at 21.5 cal ka 160 BP may represent BBDC2 (21 cal ka BP; Simon et al., 2016) although it is not associated 161 with a coarse clast-rich interval as would be expected if it represented a BBDC event 162 (Andrews et al., 1998; Simon et al., 2012; Jackson et al., 2017) (Fig. 3). The lack of an 163 interval of high NBB and IRD below 467 cm (16.2 cal ka BP) in 12PC indicates that 164 BBDC2 and BBDC3 were not recovered in 12PC. Either these two events were not 165 deposited basin wide or the basal age of 12PC is younger than the 21 ka BP age of 166 BBDC2. Given that the deepest radiocarbon age in 12PC is 21.8 cal ka BP ( $\Delta R=140$ 167 years) and there are 3 meters of sediment below this depth in the core, we suggest it is 168 more likely that BBDC2 and 3 were not deposited basin wide. Without additional

169 information we continue with the assumption that the core base is no older than the 170 beginning of the global LGM of 26.5 ka BP (Clark et al., 2009). 171 lack in core 12PC of Baffin Bay Detrital Carbonate (BBDC) events BBDC2 and 172 BBDC3, deposited between 24.7 to 25 cal ka BP and 26.4 to 27.7 cal ka BP, respectively 173 (Simon et al., 2014). We initially built the age model assuming a marine reservoir offset 174  $(\Delta R)$  of 140±30 years based on recent work in Disko Bugt (Lloyd et al., 2011), for 175 consistency with other central West Greenland sediment core records (cf Jennings et al., 176 2014; in revision 2017; Jackson et al., 2017; Hogan et al., 2016; Sheldon et al., 2016), and 177 we note that prior to 2011, many publications used a  $\Delta R=0$  years (Andrews et al., 1998; 178 Knudsen et al., 2008). However, recognizing that the marine reservoir offset could be 179 large and variable over the time interval of 12PC and because this core extends into the 180 LGM, defined here as beginning at 26.5 ka (Clark et al., 2009) and ending at the 181 beginning of the Oldest Dryas period, 18 ka BP (Buizert et al., 2014), we used the 182 variable North Atlantic R values in Stern and Lisiecki (2013) to provide an envelope of 183 calibrated age so that we could consider the correlations of boundaries and conditions 184 recorded in the core with established climatic intervals (Fig. 3f). To accomplish this we first calibrated each date with  $\Delta R=0$  <sup>14</sup>C years, which provides the maximum age. We 185 186 then used the  $\Delta R=0$  ages to identify the appropriate 500 year bin of maximum, average 187 and minimum R values from Table S1 of Stern and Lisiecki (2013) and calibrated each of 188 the dates using these three R-values. The resulting envelope of ages, from  $\Delta R=0$  to the 189 maximum Stern and Lisiecki 2013 R-value, illustrates how the choice of ΔR affects 190 correlation of boundaries in the core with climate intervals from LGM through the YD 191 (Fig. 3f; Table 1). Regardless, these results confirm that the core contains LGM and

Heinrich Stadial 1 (aka Oldest Dryas) sediments, a key requirement for testing the ice shelf model (Hulbe et al., 1997; Álvarez-Solas et al., 2010; Marcott et al., 2011).

3.2 Foraminiferal analyses.

One-cm wide samples were weighed wet and sieved on a 63-µm screen. Material >63 µm was kept wet in a storage solution of 70% distilled water and 30% ethanol with baking soda as a buffer. Foraminifera were counted wet to prevent destruction of fragile tests that disintegrate under the stress of drying. A wet splitter was used when necessary to achieve a count of 200-300 benthic formaminifers and as many planktic foraminifers as were in the benthic split. In most cases the full sample was counted. Equivalent dry weights of the foram samples were estimated from sedimentology samples from the same depths that had both wet and dry weights, allowing foraminifera/gram sediment to be calculated.

3.3 Stable isotope analyses

Stable oxygen and carbon isotopes were measured on the planktic foram species  $Neogloboquadrina\ pachyderma\$ picked from the 150-250  $\mu$ m size fraction in 41 samples; results from 3 samples were rejected because they yielded a low signal. Samples >100  $\mu$ g have standard deviations of 0.01 and 0.03 % for  $\delta^{13}$ C and  $\delta^{18}$ O respectively. Samples weighing <100  $\mu$ g are reported with a standard deviation of 0.06 % for  $\delta^{13}$ C, and an error of  $\pm 0.2$  % for  $\delta^{18}$ O. The oxygen isotope values are expressed as % vs VPDB. Between 1050 and 857 cm all samples were of small weight but otherwise seemed reliable. Measurements were made on a Micromass IsoprimeTM dual inlet coupled to a

MulticarbTM system at the Light Stable Isotope Geochemistry Laboratory at the University of Montréal – UQAM.

218 3.4 CT scan.

CT scanning of the half round core was performed at the sediment core laboratory at the University of Quebec at Rimouski. A CT number (a measure of sediment density) was extracted from the images. The CT scan image was used to determine lithofacies and boundaries, sedimentary structures, and to identify bioturbation, a key source of evidence for the presence of benthic organisms and a source of information about sedimentation rate variations between the radiocarbon dates (Wetzel, 1991). Counts of >2 mm clasts interpreted as ice rafted detritus (IRD) were made from the CT images by counting in a 2 cm wide window across the core width continuously along the core length (Grobe, 1987).

3.5 Biomarkers: IP<sub>25</sub> and Brassicasterol

Biomarker analyses (IP<sub>25</sub> and brassicasterol) were performed using methods described previously (Belt et al., 2012; Belt et al., 2015). Briefly, 9-octylheptadec-8-ene (9-OHD,  $10~\mu L$ ;  $10~\mu g~m L^{-1}$ ) and  $5\alpha$ -androstan-3 $\beta$ -ol ( $10~\mu L$ ;  $10~\mu g~m L^{-1}$ ) were added to ca. 1-2 g of each freeze-dried sediment sample prior to extraction to permit quantification of IP<sub>25</sub> and sterols, respectively. Samples were then extracted using dichloromethane/methanol (3~x~3~m L; 2:1~v/v) and ultrasonication. Following removal of the solvent from the combined extracts using nitrogen, the resulting total organic extracts (TOE) were purified using column chromatography (silica) with IP<sub>25</sub> (hexane; 6~m L) and brassicasterol (20:80~m c) methylacetate/hexane; 6~m L) collected as two single fractions. Non-polar lipid fractions

were further separated into saturated and unsaturated hydrocarbons using glass pipettes containing silver ion solid phase extraction material (Supelco Discovery® Ag-Ion). Saturated hydrocarbons were eluted with hexane (1 mL), while unsaturated hydrocarbons (including IP<sub>25</sub>) were eluted with acetone (2 mL). All fractions were dried under a stream of nitrogen.

Analysis of individual fractions was carried out using gas chromatography - mass spectrometry (GC-MS) with operating conditions as described previously (e.g. Belt et al., 2012; Brown and Belt, 2012). Sterols were derivatized (BSTFA; 50  $\mu$ L; 70 °C; 1 h) prior to analysis by GC-MS. Mass spectrometric analysis was carried out in total ion current (TIC) and single-ion monitoring (SIM) modes. Individual lipids were identified on the basis of their characteristic GC retention indices and mass spectra obtained from standards. Quantification of IP<sub>25</sub> was achieved by dividing its integrated GC-MS peak area by that of the internal standard (9-OHD) in SIM mode (both m/z 350) and normalizing this ratio using an instrumental response factor (obtained from laboratory standards of each analyte) and the mass of sediment (Belt et al., 2012). Analytical reproducibility (6 %, n = 3) was monitored using a sediment with a known concentration of IP<sub>25</sub>. Brassicasterol concentrations were obtained by comparison of their respective peak areas in SIM mode (brassicasterol, m/z 470) with those of the internal standard (m/z 333) and normalized as per IP<sub>25</sub>.

3.6 Quantitative X-ray diffraction Mineralogy

Quantitative x-ray diffraction (qXRD) analyses were used to identify shifts in sediment sources between more 'local' West Greenland (WG) and 'distal' Northern Baffin Bay

(NBB). Samples for qXRD analysis were taken at 10 to 20 cm intervals throughout the core. Sediment samples were freeze-dried and processed at INSTAAR using the method described by Eberl (2003) and Andrews and Eberl (2011). The qXRD samples were analysed on a Siemens D5000 XRD unit at a 0.02 2-θ step with a 2 second count; minerals were identified using the program RockJock v.6 (Eberl, 2003). The qXRD 2source data to 17.5 cal ka BP is presented in Jennings et al. (in revision 2017). The determination of sediment provenance is based on the quantitative X-ray diffraction (qXRD) analysis of the < 2 mm surface and core sediments using the method outlined by Eberl (2003) and described in more detail for our area by (Andrews and Eberl, 2012; Andrews et al., 2014; O'Cofaigh et al., 2013a; Simon et al., 2014). We use the Excel macro unmixing program "SedUnMix" (first described by Eberl (2004), 2004; Andrews and Eberl, 2012) to and developed further by Andrews and Eberl (2012) to ascribe sediment mineral assemblages to probable source areas. In this present study we discriminated between two glacial derived sources; first a regional West Greenland source dominated by specific ranges in quartz, plagioclase, k-feldspars and other nonclay and clay minerals, versus a North Baffin Bay detrital carbonate source dominated by dolomite (Andrews et al., 2014; O'Cofaigh et al., 2013; Jennings et al., in revision 2017).

278

279

280

281

282

283

261

262

263

264

265

266

267

268

269

270

271

272

273

274

275

276

277

### 4. Results and Interpretation

### 4.1 Lithofacies Characteristics

There are two main lithofacies units defined by the sediment parameters in 12PC (Fig. 3). The boundary between the two units (Fig. 4b) is well expressed by an abrupt shift to lower CT# (Fig. 3A). This transition dates to 16.2 cal ka BP using  $\Delta R$ =140 years

and has been interpreted to represent the retreat of the Greenland Ice Sheet from the shelf edge (Jennings et al., in revision2017). However, the full age-envelope ranges between  $16.4~(\Delta R=0)$  to 14.0~(Max~R) ka, or, late in Heinrich Stadial 1 to the end of the Bølling (Fig. 3f). Calibrated radiocarbon dates (Fig. 3F;  $\Delta R=140$ , pink) in the lower unit range from 21.8 to 16.2~cal ka BP. The lower three radiocarbon dates fall within the LGM regardless of the marine reservoir age selected (Fig. 3F). The radiocarbon date at 571.5 cm falls within Heinrich Stadial 1 regardless of the marine reservoir age (Fig. 3F).

The lower lithofacies unit, which represents the period when the ice sheet grounding line was at or near the shelf edge, has higher magnetic susceptibility (Fig. 3C), higher-variable sand content including high weight percentage peaks (Fig. 3D) and a west Greenlandic sediment composition (Fig. 3E) but rare >2mm clasts (Fig. 3B). From the base of the core to 1022 cm<sub>3</sub> sediments are laminated mud with straight, sharp contacts defining the laminae and vertically oriented burrows (Fig. 4f). Between 1025 and 768 cm the sand content increases and stratification is disrupted by bioturbation (Fig. 3E). Stratified mud with distinct vertical burrows extends from 768 to 735 cm (Fig. 3D). From 735 cm to 688 cm sand content increases. This sandy unit is overlain by another sequence of stratified mud with distinct burrows between 688 and 630 cm. The sediment between 630 and 467 cm is bioturbated, stratified mud with layering disturbed by bioturbation (Fig. 4c). The uppermost part of this unit has high sand content and marks the transition to the upper lithofacies unit.

The upper lithofacies from 467 to 0 cm, which represents deglaciation and the Holocene (Jennings et al., in revision2017), has overall lower CT number (lower density) (Fig. 3A), lower magnetic susceptibility (Fig. 3C) and generally lower sand content (Fig.

3D). But, it has much higher numbers of >2mm clasts (IRD) (Fig. 3B). Immediately above the boundary the sediments are low-density bioturbated mud with the sand fraction comprising Coscinodiscus planktic diatoms and setae of Chaetoceras, consistent with the low MS values (Fig. 3c). Well-defined, thin laminae and rare IRD occur at the base of the unit, but transition upward to less-well defined laminae and rare to absent IRD from 420 cm to 352 cm. This fine interval was interpreted to record a period in the initial deglaciation as the grounding line retreated off the shelf edge with retention of an ice shelf (Jennings et al., in revision 2017). At 352 cm (marked by middle horizontal blue line on Figure 3) the CT # (density), MS and sand increase and a spike in Greenlandic IRD occurs at 330 cm (Fig. 3A3A, B, C, DE). This level marks the start of renewed retreat of the GIS grounding line by calving (Jennings et al., in revision 2017).) - The sediments are bioturbated but stratification is still evident, suggesting moderate sedimentation rates. Apart from a peak in >2mm clasts of west Greenland provenance at 330 cm<del>The CT#, MS</del> and sand values increase to moderate levels at 355 cm (Fig. 3A, B, C) but the main rise in >2mm clasts coincides with the entry of the and Northern Baffin Bay sediment source (NBB source) content do not increase untilat 290 cm (Fig. 3B, E). The relatively low MS is consistent with the high detrital carbonate content of the NBB source (Fig. 3C, E). Bioturbated, pebbly mud associated with a rise in NBB provenance occurs between 280 and 175 cm with the highest IRD interval from 280-240 cm (Fig. 3B, E). This NBB DC interval has been found in several cores on the central West Greenland slope (Sheldon et al., 2016; Jennings et al., in revision 2017; Jackson et al., 2017) and has been correlated to BBDC1 (Simon et al., 2012; 2014; Jackson et al., 2017), marking the retreat of NBB ice streams. The NBB DC event is overlain by bioturbated mud with small, dispersed IRD

307

308

309

310

311

312

313

314

315

316

317

318

319

320

321

322

323

324

325

326

327

328

and discontinuous silt stringers between 175 and 152 cm. Bioturbated pebbly mud between 152 and 52 cm has high NBB provenance between 160 and 90 cm, an interval that contains an age reversal and a mixture of radiocarbon ages (Fig. 3F). The age reversal suggests that the upper NBB peak is reworked. The upper 52 cm of the core is bioturbated mud with dispersed IRD likely represents the middle to late Holocene time period, although it is undated.

### 4.2 Biological Proxies

Biological proxy data are expressed against age using the age model based on  $\Delta R$ =140 yrs (Fig. 5).

# 4.2.1 Bioturbation

The CT scan image (Fig. 3) reveals that the entire core is bioturbated, except for one-short interval in the LGM from 974 to 1005 cm, indicating that there was sufficient oxygenation and food to support the benthos in Baffin Bay throughout the time period represented by the core (Löwemark et al., 2012). Variations in burrow shape and density are indicative of the interplay between oxygenation, sedimentation rate, sedimentation processes, substrate consistency and food supply (Reineck and Singh, 1980, Wetzel, 1991; Löwenmark et al., 2012) (Fig. 4). Intensely bioturbated intervals in which sand layers are disrupted by burrowing (e.g. Fig. 4a, c, e) suggest periods of relatively slow sedimentation (Wetzel, 1991), whereas intervals of vertical burrows terminated by overlying strata (e.g. Fig. 4d, f) indicate episodic rapid sedimentation (Jennings et al., 2011a). Figure 4 shows expanded views of segments of the CT image shown in full on Figure 3 to illustrate some of the key lithofacies characteristics and trace fossil types that

provide evidence for sedimentation processes. Muddy intervals typically have vertical burrows that are truncated by subsequent strata (Fig. 4d). These mud intervals likely represent plumites deposited from turbid meltwater plumes, whereas the sandy, stratified intervals with varying degrees of bioturbation likely represent distal turbidites (Ó Cofaigh and Dowdeswell, 2001) (Fig. 4c, f).

4.2.2 Foraminifera and Stable Isotopes

The Foraminiferal abundances in 12PC are spiky, with intervals of low benthic and planktic numbers per gram of dry sediment punctuated by periods of much higher numbers of foraminifers per gram (Fig. 5D). The high variability in abundance relates to variations in marine productivity, overprinted by carbonate dissolution, and dilution by high (12.8 cm/ka on average from 250-860 cm) and varying sedimentation rates. The lithofacies characteristics suggest widely varying sedimentation rates in the core that are not captured by the less frequent age control. Therefore we did not attempt to calculate foraminiferal flux, which would have been a more direct measure of productivity, but rather rely on foraminiferal numbers per gram as a measure of productivity.

N. pachyderma, the only planktic species, forms abundance spikes up to 1620 specimens/g, with intervening periods of very low abundance to absence (Fig. 5). The planktic forams were quite small from the base of the core to 860 cm (22 cal ka BP), but increased in size above that level. In general the planktic and benthic foram abundances rise and fall together, suggesting that the abundance spikes represent in situ productivity and a link between surface productivity and benthic food supply, although we cannot control for variations in carbonate preservation. Low numbers of N. pachyderma per gram are consistent with low productivity under perennial sea ice and the high numbers

per gram are consistent with periods of more open water, such as leads or polynyas in summer (e.g. Nørgaard-Pedersen et al., 2003). Advection of planktic foraminifers from outside Baffin Bay is unlikely, especially given the linkage between the benthic and planktic productivity (cf Knutz et al., 2011; Nørgaard-Pedersen et al., 2003).

Oxygen isotope values on *N. pachyderma* ranged between 5.4 and 2 ‰. The interval between 22 and 18.2 cal ka BP has mostly heavy values that fall between 4 and 5 ‰ (Fig. 5), comparable to MIS 2 values in the Fram Strait (Nørgaard-Pedersen et al., 2003). A shift to lighter  $\delta^{18}$ O and  $\delta^{13}$ C values begins at 18 cal ka BP, suggests reduced ventilation (Sarnthein et al., 1995). This interval falls within HS1 regardless of which  $\Delta$ R is applied (Fig. 2; Table 1). Above this shift the  $\delta^{18}$ O values remain above 3.7 ‰. A pronounced light  $\delta^{18}$ O spike at 19.4 cal ka BP corresponds to high planktic abundance and increased IP<sub>25</sub> and Brassicasterol (Fig. 5). Oxygen isotopic values of this magnitude can either be related to glacial meltwater, especially if they are paired with light  $\delta^{13}$ C values (Sarnthein et al., 1995) or to increased rate of sea-ice production that can produce brines with a light isotopic signature (Hillaire-Marcel et al., 2004; Hillaire-Marcel and de Vernal, 2008). The overall trend in the  $\delta^{13}$ C values is toward heavier values suggesting better ventilation at the top of the record than at the bottom (Fig. 5).

The benthic foraminiferal assemblages (Fig. 6) provide insights into the productivity of surface waters, stratification of the water column, and turbid glacial meltwater influx. For example, sea-ice edge migration, either seasonal or in the form of leads or polynyas, produces pulses of phytoplankton production that sink to the seabed, providing food for benthic communities. The three most common benthic foraminiferal species in 12PC are *Stainforthia feylingi*, *Cassidulina reniforme* and *Elphidium* 

excavatum forma clavata. S. feylingi is dominant in conditions of stratified water column with a cold freshwater lid and has been associated with productivity at the seasonal sea ice edge (Seidenkrantz, 2013). It has been found in high abundances associated with biosiliceous sediments (Jennings et al., 2006). E. excavatum and C. reniforme occur together in glacial marine settings (Hald and Korsun, 1997). C. reniforme is also considered to represent chilled Atlantic Water (Slubowska et al., 2005) and is found in areas of relatively high, stable salinities (Polyak et al., 2002). E. excavatum is an opportunistic species that thrives in unstable environmental conditions influenced by rapid sedimentation and fluctuating salinities from turbid meltwater plumes (Hald and Korsun, 1997). The agglutinated species, Spiroplectammina biformis, which occurs mainly in the lower lithofacies unit is found in arctic fjords with strong meltwater signal (Jennings and Helgadottir, 1994; Schaffer and Cole, 1986). Several species indicative of marine productivity associated with nutrient rich Atlantic Water occur in both the lower and upper lithofacies unit: *Melonis barleeanus*, Buccella frigida, Nonionella turgida and Nonionellina labradorica. Islandiella norcrossi and I. helenae both are arctic species, but I. helenae is associated with sea-ice edge productivity while I. norcrossi reflects chilled Atlantic Water of normal marine salinity (Polyak et al., 2002; Wollenburg et al., 2004; Lloyd, 2006). *I. norcrossi* is a common calcareous species on the west Greenland shelf associated with Atlantic Water in the West Greenland Current (e.g. Lloyd, 2006; Perner et al., 2012). Near the top of the lower unit (16.5 cal ka BP), and continuing into the base of the overlying biosiliceous mud, several species associated with marine productivity and

nutrient rich Atlantic Water spike to high percentages. These include N. turgida, M.

399

400

401

402

403

404

405

406

407

408

409

410

411

412

413

414

415

416

417

418

419

420

422 barleeanus, B. frigida, I. norcrossi and very low percentage of Pullenia bulloides. 423 Current indicator species, Cibicides lobatulus also increases at this boundary. The central 424 part of the diatom-rich mud is barren of calcareous foraminifers and is characterized by 425 low faunal abundances dominated by agglutinated foraminiferal species (e.g. Textularia 426 earlandi), suggesting that dissolution of carbonate likely overprinted the assemblages. 427 The upper part of the <u>diatom-rich</u> mud shows a return of several of the marine 428 productivity species along with increased percentages of *P. bulloides*, a chilled Atlantic 429 water species, that is common on the SE Greenland and Northern Iceland shelves under 430 conditions of strong Irminger Current Atlantic water inflow (Eiríksson et al., 2000; 431 Jennings et al., 2011b). 432 Above the <u>diatom-rich</u> mud, the percentages of *N. labradorica* and *I. norcrossi* 433 increase, and S. feylingi continues with high percentages. The chilled Atlantic Water 434 species, Cassidulina neoteretis, is abundant at the top of the dated section along with I. 435 norcrossi, consistent with intermediate Atlantic Water and less prominent glacial 436 meltwater influence (Jennings and Helgadottir, 1993). The gap in foraminifers between 437 12 and 13.9 cal ka BP is likely a consequence of carbonate dissolution as other cores 438 from the central West Greenland margin, but in slightly shallower water (JR175-VC29; 439 Fig. 1) have C. neoteretis continuously between 14 and 11 cal ka BP (Jennings et al., in 440 revision2017). 441 4.2.3 Biomarkers 442 Further evidence of marine productivity and sea ice comes from the algal biomarkers 443 brassicasterol and IP<sub>25</sub> (Fig. 5). In general, the presence of IP<sub>25</sub> indicates release from 444 melting seasonal sea ice (Fahl and Stein, 2012; Belt et al., 2013), while the absence of

IP<sub>25</sub> is consistent with intervals of thick perennial sea ice cover or no ice cover at all (Fahl and Stein, 2012). Brassicasterol implies productivity in open-water conditions, but it also can come from melting sea ice (Belt et al., 2013). In addition, the occurrence of polynyas has been given as a possible reason for presence of IP<sub>25</sub> and brassicasterol under otherwise heavy ice conditions, even in the central Arctic Ocean (Xiao et al., 2013).

In the lower, high CT lithofacies unit of 12PC, brassicasterol and IP<sub>25</sub> are present in low abundances from 26 to 22 ka ( $\Delta R$ =140 yrs), coinciding with low foraminiferal abundances (Fig. 5). Between 22 and 20 ka, brassicasterol rises but IP<sub>25</sub> is low to absent. Foraminiferal abundances rise in this interval and the benthic fauna is characterized by productivity species (*B. frigida*, *I. helenae*, *M. barleeanus* and *N. labradorica*). An overall rise in IP<sub>25</sub> and a large peak in brassicasterol occur at 19.5 ka, and continue with moderate values until another rise in brassicasterol values within the biosiliceous diatomrich mud unit (16.2 to 15.1 cal ka BP). Both IP<sub>25</sub> and brassicasterol continue to rise after 15.1 cal ka BP, but IP<sub>25</sub> in particular rises to values unprecedented in the core after 14.3 cal ka BP.

This pattern of presence of IP<sub>25</sub> and brassicasterol in the lower lithofacies unit argues for seasonal sea ice and some open water, although the generally low concentrations suggest that these were both likely less than in the upper unit - probably due to more extensive ice cover and only periodic opening - possibly as leads or polynyas. As the final increase in IP<sub>25</sub> beginning at 16.2 ka is accompanied by rising, high brassicasterol it likely points to development of a marginal ice zone where there is increased marine productivity with probably more seasonal sea ice presence than before.

### 5. Discussion

468

469

471

473

475

477

481

483

485

487

5.1 Did an LGM Ice Shelf cover Baffin Bay?

470 There has been limited research on the LGM within Baffin Bay, which explains how the Baffin Bay ice shelf concept has remained untested. Radiocarbon dates on 472 planktic foraminifers indicate that other cores besides 12PC have planktic fauna in the LGM. Andrews et al (1998) obtained a pair of AMS <sup>14</sup>C dates from abundant planktic 474 for a minifera in southern Baffin Bay core HU77029-017PC (17,990  $\pm$  110, and 17,930  $\pm$ 210 <sup>14</sup>C yrs; Andrews et al., 1998) (Fig. 1). These <sup>14</sup>C ages calibrate to the LGM (~21 ka 476 BP;  $\Delta R=140$  years). A <sup>14</sup>C date on planktic foraminifers from core HE006-4-2PC (21,440± 140 <sup>14</sup>C yrs) on the northern side of the Uummannag TMF (Fig. 1) calibrates to 478 ~25 ka BP ( $\Delta R$ =140 years) (Ó Cofaigh et al., 2013a). In the LGM interval of 12PC (1130 479 cm to at least 690 cm) when the modeled Baffin Bay ice shelf would be in place, there 480 are multiple lines of evidence for biological activity, including bioturbation, algal biomarkers and benthic and planktic foraminifers (Figs. 3 - 6). These findings are 482 consistent with perennial sea-ice cover with some open water in the form of leads or polynyas on the eastern side of Baffin Bay. Full ice-shelf cover from an ice shelf 484 extending from the Hudson Strait ice stream and grounding on Davis Strait all the way to Greenland (Alvarez-Solas et al., 2010; 2011; Marcott et al., 2011) would not allow the 486 surface productivity (e.g. algal biomarkers, planktic forams) in Baffin Bay that would be needed to feed the benthic organisms that are evident (bioturbation and benthic 488 foraminifers). On this basis we reject the modeling result of a full Baffin Bay ice shelf. 489 While life has been observed under modern ice shelves in Antarctica, it is dependent on 490 strong ocean inflow to the sub ice-shelf cavity from outside the ice shelf (Post et al.,

2014). In the case of the Baffin Bay ice shelf cover as it is modeled, it would be sealed from the Labrador Sea marine advection and food supply.

The idea of the Davis Strait grounded ice shelf sprang in part from efforts to test a mechanism for Heinrich Event 1 (H1), in which subsurface warming reconstructed in the N. Atlantic in response to reduced Atlantic meridional overturning circulation (AMOC) during HS1 (McManus et al., 2004) weakens a buttressing ice shelf fronting the Hudson Strait ice stream and produces a Heinrich event (Álvarez-Solas et al., 2010; 2011; Marcott et al., 2011). Hulbe et al. (2004) modified their original 1997 Labrador Sea ice shelf idea to support instead fringing ice shelves along the coasts in Eastern Canada that were proposed to have met their demise through a process of meltwater infilling of surface crevasses. The existence of this type of ice shelf and H-event process has been contested (Alley et al., 2005), but it is more consistent with the 12PC data than the original idea of an ice shelf grounding on Davis Strait (Hulbe et al., 1997).

### 5.2 Heinrich Stadial Environments

The data in 12PC allow examination of the environmental response in Baffin Bay to the transition from LGM to HS1, and the response in Baffin Bay to the large ice discharge from Hudson Strait during H1 which occurred when subsurface ocean heat was at a maximum and AMOC at a minimum (Marcott et al., 2011). Locating the LGM/HS1 transition and H1 in 12PC is made difficult by the uncertainties in the magnitude of the local marine reservoir age through time (Fig. 3F) (Stern and Lisiecki, 2013). The accepted timing of H1 calving event is 16.8 ka BP (Hemming, 2004), although it may be closer to 16 ka BP based on the timing of the peak of IRD in the North Atlantic IRD stack during HS1 (Stern and Lisiecki, 2013). If we apply the ΔR envelopenvelope

approach using data from Stern and Lisiecki (2013) to the mean value of the best 2 constraining radiocarbon ages from the base of DC1 (=H1) in cores HU75009-IV-055PC and HU87033-009 LCF (Fig. 1; Andrews et al., 1994; Jennings et al., 1996), from the Labrador Sea, we obtain a range of ages for the event that spans HS1 (Table 1). The  $\Delta R$ that matches best the H1 16.8 ka age determined by Hemming (2004) is the lower  $\Delta R$ from Stern and Lisiecki (2013) (Table 1). On this basis, we chose to use the Lower  $\Delta R$  to determine where HS1 lies in the 12PC record. Lower ΔR places the base of HS1 (18 ka BP) at 610 cm and its end (14.7 ka BP) at 395cm, right at the end of the diatomaceous diatom-rich mud unit and before the initiation of calving retreat (Fig. 3F and 7). Lower  $\Delta R$  also puts the calving retreat and the timing of the west Greenland DC event (=BBDC1; Jackson et al., 2017) (Fig. 3) in the Bølling/Allerød interstadial (Fig. 7). The age model calculated with an invariant  $\Delta R=140$  years places the lithofacies transition which represents the grounding line retreat from the west Greenland shelf edge at 16.2 cal ka BP, within HS1 (Jennings et al., in revision 2017), but places the end of HS1 after the initiation of GIS calving retreat. Figure 7 illustrates how key proxy data map into the Heinrich Stadial interval defined by evidence of sluggish AMOC (McManus et al., 2004) using the lower  $\Delta R$  of Stern and Lisiecki (2013). In the Labrador Sea HS1 is an interval of anomalously warm bottom waters (Marcott et al., 2011) within which H1 occurred (Fig. 7). We would expect this massive freshwater (meltwater and icebergs) outflow from collapse of the Hudson Strait ice stream (Andrews and Tedesco, 1992; Hesse and Khodabakhsh, 2016) to perturb environments in Baffin Bay or initiate a transition to different paleoceanographic conditions.

514

515

516

517

518

519

520

521

522

523

524

525

526

527

528

529

530

531

532

533

534

535

The transition to lighter $\delta^{18}$ O values and a shift to very high percentages of <i>S</i> .
feylingi coincide with HS1 (Fig. 7). This signal is also seen in nearby core JR175-VC29
(Fig. 1), from 900 m water depth (Jennings et al., in revision 2017) and is associated in
both 12PC and VC29 with deposition of diatomaceous bioturbated diatom-rich mud with
rare IRD; a fine-grained unit of similar age is observed in core GeoTü SL-170 (Jackson et
al., 2017) slightly north of VC29. Theis diatom-rich mud interval has been interpreted by
Jennings et al. (in revision 2017) to indicate protection of the indicate exclusion of coarse
sediment delivery to the Disko TMF by retention of a fringing ice shelf Disko Trough
Mouth fan from coarse sediments released at the grounding line sediments by retreat of
the grounding line but retention of a fringing ice shelfafter initial grounding line retreat.
Overall, brassicasterol abundances are low in HS1. A period of high productivity of
benthic forams indicative of nutrient rich Atlantic water at the subsurface (Fig. 5)
(indicated on Fig. 7 by <u>red stars and the</u> -low percentages of <u>the benthic foraminiferal</u>
$\underline{\text{species}}$ , S. feylingi) coincides with the initial GIS retreat from the shelf edge as indicated
in the CT# profile (Jennings et al., in revision2017). Subsequent interstadial conditions
are marked by rising marine productivity, renewed subsurface Atlantic Water influence,
and renewed retreat of the GIS, followed by development of consistent seasonal sea ice
and release/melting of detrital carbonate bearing ice bergs from ice margins of northern
Baffin Bay <u>termed a west Greenland DC event by (Jennings et al., in revision2017) that</u>
has been shown to be correlative to BBDC1 (Simon et al. (2016) by Jackson et al. (2017).

6. Conclusions

1. Based on the data presented we reject the hypothesis that Baffin Bay was covered by a full ice shelf during the LGM. WWe conclude instead that rather than being completely covered by an ice shelf, that Baffin Bay was perennially sea-ice covered in the LGM with nutrient rich, relatively warm Atlantic water present at depth through the LGM. Evidence of marine productivity suggests that there were openings in the sea-ice cover as leads and polynyas to support marine productivity. Concurrently, sediment-laden, glacial-meltwater and turbidity currents were released from the GIS, grounded at the shelf edge, but IRD was rare suggesting the ice front was protected by a fringing ice shelf and/or the perennial sea-ice cover. 2. Reduced ventilation and productivity, coincident with a cold surface lid of meltwater was established in HS1. After Heinrich Event 1, but within the Heinrich stadial, an interval of increased productivity and Atlantic Water is associated with the retreat of the GIS grounding line from the shelf edge. 3. The implication for Heinrich Events and Ocean warming/Ice Shelf hypothesis is that perennial sea-ice cover and/or fringing ice shelves may be sufficient to explain the heat retention and back-pressure proposed to explain the dynamics that produce Heinrich Events. 7. Acknowledgements Funding for this research was provided by the US National Science Foundation grant ARC1203492 and the UK Natural Environment Research Council grant NE/D001951/1. We thank the captain, crew and scientists aboard the 2008 CSS Hudson cruise HU2008-029 for acquisition of core 2009029-12PC. We gratefully acknowledge the microscope

559

560

561

562

563

564

565

566

567

568

569

570

571

572

573

574

575

576

577

578

579

580

582 and x-ray diffraction research by undergraduate research assistants, Brian Shreve, 583 Jennifer Kelly, Matthew Reed, and Matthew Glasset. We thank Quentin Simon and one 584 anonymous reviewer for helpful critique of the manuscript. 585 586 8. Figure Captions 587 Figure 1. Bathymetric map centered on Baffin Bay (BB) showing the location of core 588 HU2008029-12PC (12PC) and other cores mentioned in the text, the distribution of 589 Paleozoic carbonate bedrock, mapped ice margin positions in northern Baffin Bay (Li et 590 al., 2011) and central west Greenland (Ó Cofaigh et al., 2013a) and major ice streams. 591 UIS = Uummannag ice stream; DIS = Disko ice stream; SSIS = Smith Sound ice stream; 592 LSIS = Lancaster Sound ice stream. Northward flowing West Greenland Current (WGC) 593 is shown as the thin red line and the southward flowing Baffin Current (BC) is shown as 594 a thin blue line. The position of the acoustic profile in Figure 2 is shown as a black line. 595 HU2008029-016PC=16; HE006-4-2PC=2; JR175-VC29=29; HU77029-017PC=17; 596 HU75009-IV-055PC=55 and HU87033-009 LCF=9. Inset plot shows the salinity and 597 temperature against water depth at from the same location as 2008029-12PC. 598 ASW=Arctic Surface Water; WGIW=West Greenland Intermediate Water; DBBW=Deep 599 Baffin Bay Water. 600 601 Figure 2. A. 3.5 kHz sub-bottom profile over the site of 2008029-12PC demonstrationg 602 the acoustically-stratified character of the seabed in the area. B. A zoom in map of the 3.5 603 kKz sub-bottom profile and the core location shown in Figure 1. The bathymetry is from 604 GEBCO.

Figure 3. Lithological proxies and age control for 2008029-12PC. A is the CT image
against depth in the core. Black bars along depth axis show the locations of CT images
shown in Figure 4. 'V' denotes locations of vertical burrows. B. IRD counts (>2mm
clasts) from CT scan in 2 cm increments. C. CT number, a measure of density derived
from the CT image. D. Magnetic Susceptibility measure by multi sensor track (MST). E.
Weight percentage of $>63~\mu m$ sand fraction from foraminiferal samples. F. Two-source
provenance of minerals: Northern Baffin Bay (NBB, brown) vs. the local source, central
west Greenland (green). F. Depth-Age model in pink ( $\Delta R=140\pm30~yrs$ ) showing $1\sigma$ and
$2 \sigma$ uncertainties of the model. Excluded from the model are benthic foraminiferal ages
(green distributions) and outliers at 1 meter. Age envelopenvelope for other potential $\Delta R$
calibrations are shown by blue ( $\Delta R$ =0); Red, green, orange = lower, mean, and upper $\Delta R$
values from Stern and Lisiecki, (2013). Climate units are along the age scale.
Figure 4. Examples of lithofacies and bioturbation types from 2008029-12PC CT scans.
See Figure 3 for locations of these examples on the CT image of the core.
Figure 5. Biological proxies from 12PC compared with CT# plot to assist with
comparison to depth on depth in Figure 3. A. CT#; B. sea ice biomarker, IP <sub>25</sub> ; C. marine
productivity biomarker, brassicasterol; D. Benthic (blue) and planktic (red) forams per
gram of dry sediment; E. $\delta^{18}$ O of planktic foraminifer, <i>N. pachyderma</i> , blue; F. $\delta^{13}$ C of <i>N</i>
pachyderma, green.

627 Figure 6. Benthic foraminiferal species in 12PC. Green represent marine productivity 628 species; Red=Atlantic Water species; Blue = Arctic species; Light Blue; Glacial marine 629 species; Orange=transformed (cooler and slightly lower salinity) Atlantic Water species. 630 631 Figure 7. Comparison between Pa/Th record of AMOC (McManus et al., 2004) and the 632 timing of Heinrich Event 1 (H1) to key paleoenvironmental proxies in 12PC. The HS1 633 interval (yellow box) is defined in the core with use of the Lower  $\Delta R$  of Stern and 634 Lisiecki (2013) (Fig. 3f). Blue lines show where key events in the core map into the 635 climatic intervals with use of the Lower  $\Delta R$  of Stern and Lisiecki (2013). A. CT # from 636 12PC; B. Brassicasterol, 12PC; C. IP<sub>25</sub>, 12PC; D. Stainforthia feylingi, 12PC; E. Oxygen 637 isotope ratios, 12PC; F. Pa/Th ratios (McManus et al., 2004). 638 References Cited 639 640 Aksu, A. E., 1985. Climatic and oceanographic changes over the past 400,000 years: 641 Evidence from deep-sea cores on Baffin Bay and David Strait. In Andrews, J. T. (ed.), 642 Quaternary Environments: Eastern Canadian Arctic, Baffin Bay and Western 643 Greenland. Boston: Allen and Unwin, 181-209. 644 645 Alley, R. B., Andrews, J. T., Barber, D. C., and Clark, P. U., 2005: Comment on 646 "Catastrophic ice shelf breakup as the source of Heinrich event icebergs" by C.L. 647 Hulbe et al. *Palaeoceanography*, 20: doi:10:1029/2004PA001086. 648 649 Álvarez-Solas, J., Charbit, S., Ritz, C., Paillard, D., Ramstein, G., and Dumas, C.: Links 650 between ocean temperature and icebergdischarge during Heinrich events, Nature 651 Geoscience, 3, 122–126, 2010 652 653 Álvarez-Solas, J., Montoya, M., Ritz, C., Ramstein, G., Charbit, S., Dumas, C., 654 Nisancioglu, K., Dokken, T., Ganopolski, A., 2011. Heinrich event 1: an example of dynamical ice-sheet reaction to ocean changes. *Climate of the Past* 7, 1297-1306. 655 656 doi:10.5194/cp-7-1297-2011. 657 658 Andrews, J.T., Eberl, D.D., 2011. Surface (sea floor) and near-surface (box cores) 659 sediment mineralogy in Baffin Bay as a key to sediment provenance and ice sheet 660 variations. Can. J. Earth Sci. 48 (9), 1307 - 1328. http://dx.doi.org/10.1139/-11-021.

- Andrews, J.T., Eberl, D.D., 2012. Determination of sediment provenance by unmixing
- the mineralogy of source-area sediments: The "SedUnMix" program. *Marine Geology*
- 664 291, 24-33.

- Andrews, J.T., Erlenkeuser, H., Tedesco, K., Aksu, A., Jull, A.J.T., 1994. Late Quaternary
- 667 (Stage 2 and 3) Meltwater and Heinrich events, NW Labrador Sea. *Quaternary*
- 668 Research 41, 26-34.

669

- Andrews, J.T, Gibb, O.T., Jennings, A.E., Simon, Q., 2014. Variations in the provenance
- of sediment from ice sheets surrounding Baffin Bay during MIS 2 and 3 and export
- to the Labrador Shelf Sea: site HU2008029-0008 Davis Strait. *Journal of Quaternary*
- 673 *Science* 29, 3-13.

674

- Andrews, J. T., Kirby, M. E., Aksu, A., Barber, D. C., and Meese, D., 1998. Late
- Quaternary Detrital Carbonate (DC-) events in Baffin Bay (67° 74° N): Do they
- 677 correlate with and contribute to Heinrich Events in the North Atlantic? *Quaternary*
- 678 *Science Reviews,* 17: 1125-1137.

679

- Andrews, J. T. and Tedesco, K., 1992: Detrital carbonate-rich sediments,
- 681 northwestern Labrador Sea: Implications for ice-sheet dynamics and iceberg rafting
- 682 (Heinrich) events in the North Atlantic. *Geology*, 20: 1087-1090.

683

- Belt, S.T., Brown, T.A., Navarro Rodriguez, A., Cabedo Sanz, P., Tonkin, A., Ingle, R.,
- 685 2012. A reproducible method for the extraction, identification and quantification of
- the Arctic sea ice proxy IP25 from marine sediments. *Analytical Methods* 4, 705-713.

687

- Belt, S.T., Brown, T.A., Ringrose, A.E., Cabedo-Sanz, P., Mundy, C.J., Gosselin, M.,
- 689 Poulin, M., 2013. Quantitative measurement of the sea ice diatom biomarker IP25
- and sterols in Arctic sea ice and underlying sediments: Further considerations for
- palaeo sea ice reconstrucion. *Organic Geochemistry* 62, 33–45.

692

- 693 Belt, S.T., Cabedo-Sanz, P., Smik, L., Navarro-Rodriguez, A., Berben, S.M., Knies, J.,
- Husum, K., 2015. Identification of paleo Arctic winter sea ice limits and the marginal
- 695 ice zone: Optimised biomarker-based reconstructions of late Quaternary Arctic sea
- ice. Earth and Planetary Science Letters 431, 127-139.

697

- Blake, W., Jr. 1977. Glacial sculpture along the east-central coast of Ellesmere Island.
- 699 Arctic Archipelago. Current Research, Part C, Geological Survey of Canada, Paper 77-
- 700 1C, 107-115.

701

- Briner, J. P., Miller, G. H., Davis, P. T., Bierman, P. R., and Cafee, M., 2003. Last Glacial
- 703 Maximum ice sheet dynamics in Arctic Canada inferred from young erratics perched
- on ancient tors. *Quaternary Science Reviews*, 22: 437-444.

- 706 Brown, T.A., Belt, S.T., 2012. Closely linked sea ice-pelagic coupling in the Amundsen
- Gulf revealed by the sea ice diatom biomarker IP25. Journal of plankton research 34,
- 708 647-654.

- Buch E. 2000a. A monograph on the physical oceanography of the Greenland waters.
- 711 Danish Meteorological Institute Scientific Report, 00-12.

712

Buch E. 2000b. Air-sea-ice conditions off southwest Greenland, 1981–1997. *Journal of Northwest Atlantic Fisheries Science* 26, 1–14.

715

- Buizert, C., Gkinis, V., Severinghaus, J.P., He, F., Lecavalier, B.S., Kindler, P.,
- Leuenberger, M., Carlson, A.E., Vinther, B., Masson-Delmotte, V., White, J.W.C., Liu, Z.,
- 718 Otto-Bliesner, B., Brook, E.J., 2014. Greenland temperature response to climate
- 719 forcing during the last deglaciation. Science 345, 1177-1180. DOI:
- 720 10.1126/science.1254961

721

- 722 Campbell, D C, de Vernal, A., 2009. CCGS Hudson Expedition 2008029: marine
- 723 geology and paleoceanography of Baffin Bay and adjacent areas, Nain, NL to Halifax,
- NS, August 28-September 23. Geological Survey of Canada, Open File 5989, 2009,
- 725 212 pages; 1 DVD, doi:10.4095/261330

726

- 727 Clark, P.U., Dyke, A.S., Shakun, D., Carlson, A.E., Clark, J., Wohlfarth, B., Mitrovica, J.X.,
- Hostetler, S.W., McCabe, A.M., 2009. The Last Glacial Maximum. Science 325, 710-
- 729 714.

730

- 731 Dahl-Jensen, D. and al., e., 1998: Past Temperatures Directly from the Greenland Ice
- 732 Sheet. *Science*, 282: 268-271.

733

- Darling, K. F., Kucera, M., Kroon, D., Wade, C.M., 2006. A resolution for the coiling
- direction paradox in *Neogloboquadrina pachyderma*. *Paleoceanography* 21,
- 736 PA2011, doi:10.1029/2005PA001189.

737

- de Vernal, A., Bilodeau, G., Hillair -Marcel, C., Kassou, N., 1992. Quantitative
- assessment of carbonate dissolution in marine sediments from foraminifer linings
- vs. shell ratios: example from Davis Strait, NW North Atlantic, Geology, 20: 527-530.

741

- Domack, E.W., Harris, P.T., 1998. A new depositional model for ice shelves, based
- upon sediment cores from the Ross Sea and the Mac. Roberson shelf, Antarctica.
- 744 *Annals of Glaciology* 27, 281-284.

745

- Dowdeswell, J.A., Hogan, K.A., Ó Cofaigh, C., Fugelli, E.M.G., Evans, J., Noormets, R.,
- 747 2014. Late Quaternary ice flow in aWest Greenland fjord and cross-shelf trough
- system: submarine landforms from Rink Isbrae to Uummannag shelf and slope.
- 749 *Quat. Sci. Rev.* 92, 292-309. http://dx.doi.org/10.1016/j.quascirev.2013.09.007.

- 751 Dyke, A. S., Andrews, J. T., Clark, P. U., England, J. H., Miller, G. H., Shaw, J., and
- 752 Veillette, J. J., 2002: The Laurentide and Innuitian ice sheets during the Last Glacial
- 753 Maximum. *Quaternary Science Reviews*, 21, 9-31.

- Eberl, D.D., 2003. User guide to RockJock: A program for determining quantitative
- 756 mineralogy from X-ray diffraction data. United States Geological Survey, Open File
- 757 Report 03-78, 40 pp, Washington, DC.

758

- 759 Eiríksson, J., Knudsen, K.L., Haflidason, H., Henriksen, P., 2000. Late-glacial and
- Holocene palaeoceanography of the North Icelandic shelf. Journal of Quaternary
- 761 *Science* 15, 23-42.

762

- 763 England, J. 1999. Coalescent Greenland and Innuitian ice during the Last Glacial
- 764 Maximum: Revising the Quaternary of the Canadian High Arctic. *Quaternary Science*
- 765 *Reviews* 18, 421–426, <a href="http://dx.doi.org/10.1016/S0277-3791(98)00070-5">http://dx.doi.org/10.1016/S0277-3791(98)00070-5</a>.

766

- England, J., Atkinson, N., Bednarski, J., Dyke, A.S., Hodgson, D.A., Ó Cofaigh, C. 2006.
- The Innuitian Ice Sheet: configuration, dynamics and chronology. *Quaternary*
- 769 *Science Reviews* 25, 689-703.

770

- 771 Fahl, K., Stein, R., 2012. Modern seasonal variability and deglacial/Holocene change
- of central Arctic Ocean sea ice cover: New insights from biomarker proxy records.
- 773 Earth and Planetary Science Letters 351–352, 123–133.

774

- Grobe, H., 1987. A simple method for the determination of ice-rafted debris in
- sediment cores. *Polarforschung* 57 (3), 123-126.

777

- Hald, M., Korsun, S. 1997. Distribution of modern benthic foraminifera from fjords of
- 779 Svalbard, European Arctic. *Journal of Foraminiferal Research* 27, 101–122.

780

- Hemming, S.R., 2004. Heinrich events: massive late Pleistocene detritus layers of the
- North Atlantic and their global climate imprint. *Rev. Geophys.* 42, RG1005.

783

- Hesse, R., Khodabakhsh, S. 2016. Anatomy of Labrador Sea Heinrich layers. *Marine*
- 785 *Geology* 380, 44-86. http://dx.doi.org/10.1016/j.margeo.2016.05.019

786

- Hesse, R., Khodabakhsh, S., Klaucke, I., Ryan, WBF., 1997. Asymmetrical turbid
- surface-plume deposition near ice-outlets of the Pleistocene Laurentide ice sheet in
- the Labrador Sea. *Geo-Marine Letters*, 17, 179-187.

790

- Hillaire-Marcel, C., de Vernal, A., 2008. Stable isotope clue to episodic sea-ice
- 792 formation in the glacial North Atlantic. Earth and Planetary Science Letters, 268.
- 793 143-150.

- Hillaire-Marcel, C., de Vernal, A., Aksu, A.E., Macko, S., 1989. High-resolution
- 796 isotopicand micropaleontological studies of upper Pleistocene sediments at ODP
- 797 Site 645, Baffin Bay, Proceedings of the Ocean Drilling Program, 105B: 599-616.

- Hofmann, J.C., Knutz, P.C., Nielsen, T., Kuijpers, A., 2016. Seismic architecture and evolution of the Disko Bay trough-mouth fan, central West Greenland margin,
- 801 *Quaternary Science Reviews*, http://dx.doi.org/10.1016/j.quascirev.2016.05.019

802

- Holland, D.M., Thomas, R.H., de Young, B., Ribergaard, M.H., Lyberth, B., 2008.
- 804 Acceleration of Jakobshavn Isbræ triggered by warm subsurface oceanwaters.
- 805 *Nature Geoscience* 1 (10), 659**e**664. http://dx.doi.org/10.1038/ngeo316.

806

Hulbe, C.L., 1997. An ice shelf mechanism for Heinrich layer production, *Paleoceanography* 12, 711 –717.

809

- Hulbe, C. L., MacAyeal, D. R., Denton, G. H., Kleman, J., and Lowell, T. V., 2004:
- Catastrophic ice shelf breakup as the source for Heinrich event icebergs.
- 812 *Palaeoceanography,* 19: 1 of 15, doi.10.1029/2003:PA000890, 002004.

813

- Jackson, R., Carlson, A.E., Hillaire-Marcel, C., Wacker, L., Vogt, C., Kucera, M., 2017.
- Asynchronous instability of the North American-Arctic and Greenland ice sheets
- during the last deglaciation. *Quaternary Science Reviews* 164, 140-153.
- 817 http://dx.doi.org/10.1016/j.quascirev.2017.03.020.

818

- Jennings, A.E., Andrews, J.T., Ó Cofaigh, C., St. Onge, G., Sheldon, C., Belt, S.T., Cabedo-
- Sanz, P., Hillaire-Marcel, C. in revision 2017. Ocean forcing of Ice Sheet Retreat in
- Central West Greenland from LGM through Deglaciation. *Earth and Planetary Science Letters* 472, 1-13.
- 022

823

- Jennings, A.E., Andrews, J.T., Wilson, L., 2011b. Holocene Environmental Evolution of
- the SE Greenland Shelf North and South of the Denmark Strait: Irminger and East
- 826 Greenland Current Interactions. Quaternary Science Reviews 30: 980-998.

827

- Jennings, A.E., Hald, M., Smith, L.M., and Andrews, J.T., 2006. Freshwater forcing
- from the Greenland Ice Sheet during the Younger Dryas: Evidence from
- 830 southeastern Greenland shelf cores: *Quaternary Science Reviews* 25, 282–298,
- 831 doi:10.1016/j.quascirev.2005.04.006.

832

- Jennings, A.E., Helgadottir, G., 1994. Foraminiferal assemblages from the fjords and
- shelf of eastern Greenland. *J. Foraminifer. Res.* 24 (2), 123e144.
- 835 http://dx.doi.org/10.2113/gsjfr.24.2.123.

836

- 837 Jennings, A.E., Sheldon, C., Cronin, T.M., Francus, F., Stoner, J., Andrews, J., 2011a. The
- 838 Holocene history of Nares Strait, transition from glacial bay to Arctic-Atlantic
- throughflow. *Oceanography* 24, no. 3, 26-41.

- Jennings, A. E., Tedesco, K. A., Andrews, J. T., and Kirby, M. E., 1996. Shelf erosion and
- glacial ice proximity in the Labrador Sea during and after Heinrich events (H-3 or 4
- to H-0) as shown by foraminifera. *In* Andrews, J. T., Austin, W. E. N., Bergsten, H., and
- 844 Jennings, A. E. (eds.), Late Quaternary Palaeoceanography of the North Atlantic
- 845 *Margins*: Geological Society Special Publications, 29-49.

- Jennings, A.E., Walton, M.E., Cofaigh, C.\_O., Kilfeather, A., Andrews, J.T., Ortiz, J.D., et
- al., 2014. Paleoenvironments during Younger Dryas-early Holocene retreat of the
- Greenland ice sheet from outer Disko Trough, central west Greenland. *J. Quat. Sci.* 29
- 850 (1), 27e40. http://dx.doi.org/10.1002/jqs.2652.

851

- Kaufman, D.S., Williams, K.M. (compilers), 1992. Radiocarbon Date List VII: Baffin
- 853 Island, N.W.T., Canada. INSTAAR Occasional Paper 48. Institute of Arctic and Alpine
- 854 Research, University of Colorado, Boulder.

855

- Knutz, P. C., M.-A. Sicre, H. Ebbesen, S. Christiansen, and A. Kuijpers, 2011. Multiple-
- stage deglacial retreat of the southern Greenland Ice Sheet linked with Irminger
- 858 Current warm water transport, *Paleoceanography* 26, PA3204,
- 859 doi:10.1029/2010PA002053.

860

- Li, G., Piper, D. J. W., and Campbell, D. C., 2011: The Quaternary Lancaster Sound
- trough-mouth fan, NW Baffin Bay. *Journal of Quaternary Science*, 26: 511-522.
- Lloyd, J. M. 2006. Modern distribution of benthic foraminifera from Disko Bugt, West
- Greenland. *Journal of Foraminiferal Research* 36, 315–331.

865

- Lloyd, J.M., Moros, M., Perner, K., Telford, R.J., Kuijpers, A., Jansen, E., et al., 2011.A
- 867 100 yr record of ocean temperature control on the stability of JakobshavnIsbrae,
- 868 West Greenland. *Geology* 39 (9), 867-870. http://dx.doi.org/10.1130/G32076.1.

869

- Löwemark, L., O'Regan, M., Hanebuth, T.I.I., Jakobsson, M., 2012. Late Quaternary
- spatial and temporal variability in Arctic deep-sea bioturbation and its relation to
- 872 Mn cycles. *Palaeogeography, Palaeoclimatology, Palaeoecology* 365-366, 192-208.

873

- Lucci, RG and Rebesco, M., 2007. Glacial contourities on the Antarctic Peninsula
- 875 margin: insight for palaeoenvironmental and palaeoclimatic conditions. Geological
- 876 Society, London, Special Publications, 276: 111-127.

877

- Marcott et al., 2011. Ice-shelf collapse from subsurface warming as a trigger for
- 879 Heinrich Events. PNAS 108. No. 33 p. 13415-13419

880

- McManus, J.F., Francois, R., Gherardi, J.-M., Keigwin, L.D., Brown-Leger, S., 2004.
- 882 Collapse and rapid resumption of the Atlantic meridional circulation linked to
- deglacial climate change. Nature 428, 834-837.

- Münchow A., Falkner, A. Melling, H., 2015. Baffin Island and West Greenland Current
- 886 Systems in northern Baffin Bay. *Progress in Oceanography* 132, 305–317

- O Cofaigh C., Andrews JT, Jennings AE, Dowdeswell JA, Hogan KA, Kilfeather AA, et al. (2013a) Glacimarine lithofacies, provenance and depositional processes on a West
- 890 Greenland trough-mouth fan. Journal of Quaternary Science 28. Available at:
- 891 http://dx.doi.org/10.1002/jqs.2569: doi:10.1002/jqs.2569.

892

6 O Cofaigh C, Dowdeswell J.A., 2001. Laminated sediments in glacimarine environments: diagnostic criteria for their interpretation. *Quaternary Science Reviews* 20, 1411-1436.

895

Ó Cofaigh C., Dowdeswell J.A., Jennings A.E., Hogan K.A., Kilfeather A., Hiemstra
 J.F., et al. (2013b) An extensive and dynamic ice sheet on the West Greenland shelf
 during the last glacial cycle. *Geology* 41(2): 219–222: doi:10.1130/G33759.1.

899

Nørgaard-Pedersen, N., Spielhagen, R.F., Erlenkeuser, H., Grootes, P.M., Heinemeier, J., Knies, J., 2003. Arctic Ocean during the Last Glacial Maximum: Atlantic and polar domains of surface water mass distribution and ice cover. Paleoceanography 18, doi:10.1029/2002PA000781, 2003.

904

Perner, K., Moros, M., Jennings, A., Lloyd, J.M., Knudsen, K.L., 2012. Holocene
 palaeoceanographic evolution off West Greenland. *The Holocene* 23, 374-387.

907

Piénkowski, A.J., England, J.H., Furze, M.F.A., Marret, F., Eynaud, F., Vilks, G., Maclean,
 B., Blasco, S., Scourse, J.D., 2012. The deglacial to postglacial marine environments of
 SEBarrow Strait, Canadian Arctic Archipelago. *Boreas* 41 (2), 141-179.
 http://dx.doi.org/10.1111/j.1502-3885.2011.00227.x.

912

Polyak, L., Korsun, S., Febo, L.A., Stanovoy, V., Khusid, T., Hald, M., Paulsen, B.E.,
 Lubinski, D.J., 2002. Benthic foraminiferal assemblages from the southern Kara Sea,
 a river influenced Arctic marine environment. *Journal Foraminiferal Research* 32,
 252–273.

917

Post, A.L., Galton-Fenzi, B.K., Riddle, M.J., Herraiz-Borreguero, L., O'Brien, P.E.,
 Hemer, M.A., McMinn, A., Rasch, D., Craven, M., 2014. Modern sedimentation,
 circulation and life beneath the Amery Ice Shelf, East Antarctica. *Continental Shelf Research* 74. 77-87.

922

- Quillmann, U., Andrews, J. T., and Jennings, A. E., 2009: Radiocarbon Date List XI:
   East Greenland shelf, West Greenland Shelf, Labrador Sea. Baffin Island shelf, Baffin Bay, Nares Strait, and Southwest to Northwest Icelandic shelf. Occasional Paper No.
- 926 59, INSTAAR, University of Colorado, Boulder, Boulder.

927

Ramsey, C.B. and Lee, S., 2013. Recent and planned developments of the program OxCal. Radiocarbon 55, 720-730.

- Reeh, N., Thomsen, H. H., Higgins, A. K., and Weidick, A., 2001: Sea ice and the
- 932 stability of north and northeast Greenland floating glaciers. *In* Jeffries, M. O. and
- 933 Eicken, H. (eds.), *Annals of Glaciology, Vol 33*, 474-480.

- Reimer, P.J., Bard, E., Bayliss, A., Beck, J.W., Blackwell, P.G., Ramsey, C.B., Grootes,
- 936 P.M., Guilderson, T.P., Haflidason, H., Hajdas, I., Hatté, C., Heaton, T.J., Hoffmann,
- 937 D.L., Hogg, A.G., Hughen, K.A., Kaiser, K.F., Kromer, B., Manning, S.W., Niu, M.,
- Reimer, R.W., Richards, D.A., Scott, E.M., Southon, J.R., Staff, R.A., Turney, C.S.M.,
- van der Plicht, J., 2013. IntCal13 and Marine13 radiocarbon age calibration curves 0-
- 940 50,000 years cal BP. Radiocarbon 55, 1869–1887. http://dx.doi.org/10.2458/azu js rc.
- 941 55.16947.

942

Reineck, H.E., Singh, I.B., 1980. Depositional Sedimentary Environments. Springer-Verlag, NY.

945

- 946 Sarnthein, M., et al., Variations in Atlantic surface ocean paleoceanography, 50\_-80\_N:
- A time-slice record of the last 30,000 years, Paleoceanography, 10(6), 1063–1094, 1995.
- 948 Schafer, C.T., Cole, F.E., 1988. Environmental associations of Baffin Island fjord
- agglutinated foraminifera. Abh. Geol. Bundesanst, 307.

950

- 951 Seidenkrantz, M.-S., 2013. Benthic foraminifera as palaeo sea-ice indicators in the
- 952 subarctic realm-examples from the Labrador Sea-Baffin Bay region. *Quaternary Science*
- 953 Reviews 79, 135-144. http://dx.doi.org/10.1016/j.quascirev.2013.03.014

954

- 955 Shaffer, G., Olsen, S.M., Bjerrum, C.J., 2004. Ocean subsurface warming as a
- 956 mechanism for coupling Dansgaard-Oeschger climate cycles and ice-rafting events.
- 957 Geophysical Research Letters 31, L24202. doi:10.1029/2004GL020968.

958

- 959 Sheldon, C., Jennings, A., Andrews, J.T., Ó Cofaigh, C., Hogan, K., Dowdeswell, J.A.,
- 960 Seidenkrantz, M-S., 2016. Ice stream retreat following the LGM and onset of the west
- Greenland current in Uummannag Trough, west Greenland. *Quaternary Science Reviews*,
- 962 http://dx.doi.org/10.1016/j.guascirev.2016.01.019

963

- 964 Simon, Q., Hillaire-Marcel, C., St-Onge, G., Andrews, J.T., 2014. Northeastern
- Laurentide, western Greenland and southern Innuitian ice stream dynamics during the last
- glacial cycle. Journal of Quaternary Science 29(1): 14-26. DOI: 10.1002/jqs.2648

967

- 968 Simon Q, St-Onge G, Hillaire-Marcel C., 2012. Late Quaternary chronostratigraphic
- 969 framework of deep Baffin Bay glaciomarine sediments from high-resolution
- paleomagnetic data. Geochemistry, Geophysics, Geosystems 13: Q0AO03. doi: 10.1029/
- 971 2012GC004272

- 973 Simon, Q., Thouveny, N., Bourles, D.L., Nuttin, L., Hillaire-Marcel, C., St-Onge, G.,
- 2016. Authigenic <sup>10</sup>Be/ <sup>9</sup>Be ratios and <sup>10</sup>Be-fluxes (<sup>230</sup>Th<sub>ys</sub>-normalized) in central Baffin
- Bay sediments during the last glacial cycle: Paleoenvironmental implications. *Quaternary*
- 976 Science Reviews 140, 142-162.

- 978 Slabon, P., Dorschel, B., Jokat, W., Myklebust, R., Hebbeln, D., Gebhardt, C., 2016.
- Greenland ice sheet retreat history in the northeast Baffin Bay based on high-resolution
- 980 bathymetry. Quaternary Science Reviews 154, 182-198.
- 981 http://dx.doi.org/10.1016/j.quascirev.2016.10.022

982

- 983 Slubowska, M.A., Koç, N., Rasmussen, T.L., Klitgaard-Kristensen, D., 2005. Changes in
- 984 the flow of Atlantic water into the Arctic Ocean since the last deglaciation: evidence from
- 985 the northern Svalbard continental margin, 80 N. Paleoceanography 20, PA4014.
- 986 doi:10.1029/2005PA001141.

987

- Stern, J.V., Lisiecki, L.E. 2013. North Atlantic circulation and reservoir age changes over
- the past 41,000 years. Geophysical Research Letters 40: 3693-3697.
- 990 doi:10.1002/grl.50679, 2013.

991

- 992 Straneo, F., Sutherland, D.A., Holland, D., Gladish, C., Hamilton, G.S., Johnson, H.L.,
- Rignot, E., Xu, Y., Koppes, M., 2012. Characteristics of ocean waters reaching
- 994 Greenland's glaciers. Annals of Glaciology 53(60), 202-210.
- 995 doi:10.3189/2012AoG60A059

996

- 797 Tang, C.C.L., Ross, C.K., Yao, T., Petrie, B., DeTracey, B.M., Dunlap, E., 2004. The
- 998 circulation, water masses and sea-ice of Baffin Bay. Progress in Oceanography 63, 183-
- 999 228.

1000

- 1001 Wetzel, A., 1991. Ecologic interpretation of deep-sea trace fossil co=unities.
- Palaeogeography, Palaeoclimatology, Palaeoecology 85, 47-69.

1003

- Wollenburg, J.E., Knies, J., Mackensen, A., 2004. High-resolution paleoproductivity
- fluctuations during the past 24 kyr as indicated by benthic foraminifera in the
- marginal Arctic Ocean. Palaeogeography, Palaeoclimatology, Palaeoecology 204, 209-
- 1007 238.

1008

- 1009 Xiao, X., Fahl, K., Stein, R., 2013. Biomarker distributions in surface sediments from the
- 1010 Kara and Laptev seas (Arctic Ocean): indicators for organic-carbon sources and sea ice
- 1011 coverage. Quaternary Science Reviews 79, 40–52.

1012

- Zreda, M., J. England, F. Phillips, D. Elmore, and P. Sharma. 1999. Unblocking of the
- Nares Strait by Greenland and Ellesmere Ice-Sheet retreat 10,000 years ago. *Nature*
- 1015 398,139–142, http://dx.doi.org/10.1038/18197

- Baffin Bay was not covered by an ice shelf in the LGM.
- Baffin Bay was perennially sea-ice covered through the LGM.
- LGM marine productivity promoted by leads and polynyas in perennial sea-ice cover.
- Heinrich stadial paleoenvironments vary and are associated with GIS retreat
- H1 Ice Shelf hypothesis rejected; no evidence for Baffin Bay full ice shelf.

# Baffin Bay Paleoenvironments in the LGM and HS1: Resolving the ice-shelf question

2 3

1

- 4 Anne E. Jennings<sup>1\*</sup>, John T. Andrews<sup>1</sup>, Colm Ó Cofaigh<sup>2</sup>, Guillaume St-Onge<sup>3</sup>, Simon
- 5 Belt<sup>4</sup>, Patricia Cabedo-Sanz<sup>4</sup>, Christof Pearce<sup>5,6</sup>, Claude Hillaire-Marcel<sup>7</sup>, D. Calvin
- 6 Campbell<sup>8</sup>
- 7 INSTAAR University of Colorado, Campus Box 450, Boulder, CO 80309-0450 USA
- 8 <sup>2</sup> Department of Geography, Durham University, South Road, Durham DH1 3LE, United
- 9 Kingdom
- <sup>3</sup> Institut des sciences de la mer de Rimouski (ISMER) Université du Québec à Rimouski
- and GEOTOP Rimouski, Québec, Canada S5L 3A1
- 12 <sup>4</sup> School of Geography, Earth and Environmental Sciences, University of Plymouth,
- 13 Plymouth PL4 8AA United Kingdom
- <sup>5</sup> Department of Geological Sciences and Bolin Centre for Climate Research, Stockholm
- 15 University, Svante Arrhenius väg 8, SE-106 91 Stockholm, Sweden
- 16 6 Department of Geoscience and Arctic Research Centre, Aarhus University, Hoegh
- 17 Guldbergs gade 2, 8000 Aarhus, Denmark
- <sup>7</sup> Université du Québec a Montréal, Centre GEOTOP CP 8888, succ. Centre-Ville,
- 19 Montréal, Québec, Canada, H3C 3P8
- 20 <sup>8</sup> Geological Survey of Canada-Atlantic, Natural Resources Canada, Dartmouth Nova
- 21 Scotia
  - \* anne.jennings@colorado.edu

22 23 24

25

26

27

28

29

30 31

32

33

34

35

36 37

38

39

40

41

42

43

44

45

46

47

48 49

50

Core HU2008029-12PC from the Disko trough mouth fan on the central West Greenland continental slope is used to test whether an ice shelf covered Baffin Bay during the Last Glacial Maximum (LGM) and at the onset of the deglaciation. We use benthic and planktic foraminiferal assemblages, stable isotope analysis of planktic forams, algal biomarkers, ice-rafted detritus (IRD), lithofacies characteristics scans, and quantitative mineralogy to from CT paleoceanographic conditions, sediment processes and sediment provenance. The chronology is based on radiocarbon dates on planktic foraminifers using a  $\Delta R$  of 140 ± 30 <sup>14</sup>C years, supplemented by the varying reservoir estimates of Stern and Lisiecki (2013) that provide an envelope of potential ages. HU2008029-12PC is bioturbated throughout. Sediments between the core base at 11.3 m and 4.6 m (LGM through HS1) comprise thin turbidites, plumites and hemipelagic sediments with Greenlandic provenance consistent with processes active at the Greenland Ice Sheet margin grounded at or near the shelf edge. Abundance spikes of planktic forams coincide with elevated abundance of benthic forams in assemblages indicative of chilled Atlantic Water, meltwater and intermittent marine productivity. IRD and IP<sub>25</sub> are rare in this interval, but brassicasterol, an indicator of marine productivity reaches and sustains low levels during the LGM. These biological characteristics are consistent with a sea-ice covered ocean experiencing periods of more open water such as leads or polynyas in the sea ice cover, with chilled Atlantic Water at depth, rather than full ice-shelf cover. They do not support the existence of a full Baffin Bay ice shelf cover extending from grounded ice on the Davis Strait. Initial ice retreat from the West Greenland margin is manifested by a pronounced lithofacies shift to bioturbated, diatomaceous mud with rare IRD of Greenlandic origin at 467 cm (16.2 cal ka BP; ΔR=140 yrs) within HS1. A spike in foraminiferal abundance and ocean warmth indicator benthic forams precedes the initial ice retreat from the shelf edge. At the end of HS1, IP<sub>25</sub>, brassicasterol and benthic

forams indicative of sea-ice edge productivity increase, indicating warming interstadial conditions. Within the Bølling/Allerød interstadial a strong rise in IP<sub>25</sub> content and IRD spikes rich in detrital carbonate from northern Baffin Bay indicate that northern Baffin Bay ice streams were retreating and provides evidence for increased open water, advection of Atlantic Water in the West Greenland Current, and formation of an IRD belt along the W. Greenland margin.

57 58

Keywords: Greenland Ice Sheet, Baffin Bay, paleoceanography, ice shelf, foraminifera, Heinrich Stadial 1

59 60

# 1. Introduction

62

63

64

65

66

67

68

69

70

71

72

73

74

75

76

77

78

61

Last Glacial Maximum (LGM) climatic and oceanic conditions in Baffin Bay are currently poorly known, but according to the temperature reconstructions from the Greenland Ice Sheet borehole (Dahl-Jensen and al., 1998) and ice-core data (Buizert et al., 2014), summit temperatures were ~20°C colder than present. Applying this temperature difference down to sea level using the adiabatic lapse rate, suggests that the annual temperature at the surface of Baffin Bay adjacent to Baffin Island would approach -36°C. Such cold temperatures support the argument that cold-based ice covered the forelands of eastern Baffin Island (Briner et al., 2003) with "Antarctic-like" conditions across Baffin Bay, which would also suggest that Baffin Bay was covered in perennial sea ice. At the LGM, confluent, Innuitian (IIS), Laurentide (LIS) and Greenland (GIS) ice sheets (England et al., 2006) blocked the channels that connect Baffin Bay to the Arctic Ocean (Dyke, 2002) and terminated in northern Baffin Bay as large ice streams (Li et al., 2011; Blake, 1977). The Greenland ice sheet reached the continental shelf edge via large ice streams off west Greenland (Ó Cofaigh et al., 2013a; Jennings et al., 2017; Slabon et al., 2016; Sheldon et al., 2016; Dowdeswell et al., 2014), but the outer limits of the ice on the Baffin shelf are not known.

On the basis of modeling, it has been proposed that Baffin Bay was blocked at its
southern end by an ice shelf extension of the Hudson Strait ice stream that grounded
across Davis Strait to reach southern Greenland, thus sealing Baffin Bay from the
Labrador Sea (Hulbe et al., 1997; Álvarez-Solas et al., 2010; Marcott et al., 2011). This
ice shelf was the starting point for modeling the processes that produce Heinrich events
(Hulbe et al., 1997; Álvarez-Solas et al., 2010; Marcott et al., 2011), but physical
evidence for it has not been recovered. An ice shelf of this scale would have
environmental consequences that should be recorded in Baffin Bay sediments. Firstly,
grounding of a Labrador Sea ice shelf along Davis Strait would prevent seawater
exchange between Baffin Bay and the Labrador Sea, excluding advection of organic
matter into Baffin Bay. It also would shut down in situ primary marine productivity in
Baffin Bay so that planktic and benthic organisms, their biomarkers, and bioturbation
would be absent in the sediment. Secondly, ice shelves and even extensive sea-ice cover
are known to restrict the movement and export of icebergs (Reeh et al., 2001; Domack
and Harris, 1998). Thus iceberg rafting and mixing of sediments of various provenances
in Baffin Bay would be reduced. Using these concepts, we test the LGM Baffin Bay ice-
shelf hypothesis by studying the sedimentological and biological characteristics of
sediments in HU2008029-12PC from the continental slope off western Greenland, a core
that extends from the LGM into the Younger Dryas (YD) and that recorded retreat of the
Greenland Ice Sheet during deglaciation (Jennings et al., 2017).

# 2. Setting of core HU2008029-12PC

Detailed studies of LGM and deglacial environments in Baffin Bay have been hampered by relatively slow sediment accumulation rates and poor calcium carbonate preservation (cf. Aksu, 1985; de Vernal et al., 1992; Simon et al., 2012). HU2008029-12PC (hereafter called 12PC) was raised from the northern side of the Disko trough mouth fan (TMF) from acoustically stratified sediments with continuous parallel reflections on the eastern side of Baffin Bay (68°13.69' N; 57°37.08' W; 1475 m water depth; Campbell and de Vernal, 2009) (Figs. 1 and 2). This site on the trough mouth fan has higher sediment accumulation than sites in the deep basin of Baffin Bay that have variable sedimentation rates that range between 3 and 35 cm/ka (Andrews et al., 1998; Hillaire-Marcel et al., 1989, 2004; Simon et al., 2012; 2014) (Fig. 1).

The Disko TMF was built throughout the Quaternary by rapid sediment deposition in front of the fast flowing Disko ice stream (Fig. 1) when the GIS margin was extended on the shelf, and from hemipelagic sedimentation during and after ice retreat (ÓCofaigh et al., 2013a, b; Jennings et al., 2017; Hofmann et al., 2016). An ice sheet grounded at or near the shelf edge delivers abundant sediments directly to the continental slope in the form of sediment gravity flows, including turbidity currents that form graded sand layers, stratified sand/silt beds, and glacigenic debris flows (ÓCofaigh et al., 2013a, b, Lucci and Rebesco, 2007). Turbid meltwater plumes released from the ice front produce plumites, which are finer grained than the turbidites as the sand is dropped near the ice front and the silt and clay continue offshore in suspension (Hesse et al., 1997; Lucchi and Rebesco, 2007). Depending on sea surface conditions such as perennial sea ice and/or ice shelves, icebergs would also deliver sediment to the slope as they melted

during their transit in Baffin Bay (Andrews et al., 1998; 2014; Jennings et al., 2014; Simon et al., 2012; 2014; 2016; Sheldon et al., 2016).

The modern sea ice edge extends southeast to northwest within Baffin Bay and sea ice cover is greater in the western than in the eastern half due to the influence of the relatively warm and saline West Greenland Current that enters Baffin Bay from the southeast (Tang et al., 2004; Münchow et al., 2015) (Fig. 1). The boundary between lower salinity, sea-ice bearing, Arctic Surface Water (ASW) that passes from the Arctic Ocean through the channels of the Canadian Arctic Archipelago into Baffin Bay and Atlantic Waters of the West Greenland Current (WGC) moving northward along West Greenland is oriented NE-SW and migrates through the year. The relatively warm, saline Atlantic Water submerges beneath the ASW (Buch, 2000a, b) and forms the West Greenland Intermediate Water (WGIW) (Fig. 1 inset) (Tang et al., 2004). During the LGM, however, the circulation regime in Baffin Bay would have been different because the southward flow of ASW into Baffin Bay was blocked by confluent ice sheets grounded in the channels of the Canadian Arctic Archipelago until the early Holocene (England, 1999; Zreda et al., 1999; Jennings et al., 2011a; Piénkowski et al., 2011). Today, warm Atlantic Water carried in the WGC accesses the GIS margins via cross shelf troughs and fjords, where the ice sheet terminates in the sea (Holland et al., 2008) and promotes basal melting (Straneo et al., 2012). WGC Atlantic Water flow was initiated as early as 14.4 cal ka BP off central West Greenland and is implicated in Greenland Ice Sheet retreat from the LGM position at the shelf edge (cf. Knutz et al., 2011; Sheldon et al., 2016; Jennings et al., 2017).

145

123

124

125

126

127

128

129

130

131

132

133

134

135

136

137

138

139

140

141

142

143

# 3. Methods:

146

148

149

150

151

152

153

154

155

156

157

158

159

160

161

162

163

164

165

166

167

168

147 3.1 Age Model

The age model for 12PC is based on 7 radiocarbon dates between 201 and 860 cm on the arctic planktic foraminifer, Neogloboquadrina pachyderma (sensu Darling et al., 2006). The dates were previously published in Jennings et al., (2017) (Table 1). Radiocarbon dates were calibrated using the Marine 13 curve (Reimer et al., 2013). OxCal version 4.2.4 (Ramsey and Lee, 2013) was used to compute an age/depth model (Fig. 3). An age reversal in the upper 110 cm of the core limited the chronology to the interval from 200 cm to the base of the core (1130 cm). The age of the core base is assumed to be no older than 26.5 ka BP, the beginning of the LGM (Clark et al., 2009). This assumed basal age results in a large uncertainty in the modeled age of the base of the core (24 to 28 cal ka BP). Given this basal age, we might expect to record Baffin Bay Detrital Carbonate (BBDC) event BBDC3 that is found in central Baffin Bay from c. 23.5 to 25 cal ka BP (Simon et al., 2016). A single data point with 20% NBB source at 21.5 cal ka BP may represent BBDC2 (21 cal ka BP; Simon et al., 2016) although it is not associated with a coarse clast-rich interval as would be expected if it represented a BBDC event (Andrews et al., 1998; Simon et al., 2012; Jackson et al., 2017) (Fig. 3). The lack of an interval of high NBB and IRD below 467 cm (16.2 cal ka BP) in 12PC indicates that BBDC2 and BBDC3 were not recovered in 12PC. Either these two events were not deposited basin wide or the basal age of 12PC is younger than the 21 ka BP age of BBDC2. Given that the deepest radiocarbon age in 12PC is 21.8 cal ka BP ( $\Delta R=140$  years) and there are 3 meters of sediment below this depth in the core, we suggest it is more likely that BBDC2 and 3 were not deposited basin wide. Without additional information we continue with

the assumption that the core base is no older than the beginning of the global LGM of 170 26.5 ka BP (Clark et al., 2009).

169

171

172

173

174

175

176

177

178

179

180

181

182

183

184

185

186

187

188

189

190

191

We initially built the age model assuming a marine reservoir offset ( $\Delta R$ ) of 140±30 years based on recent work in Disko Bugt (Lloyd et al., 2011), for consistency with other central West Greenland sediment core records (cf Jennings et al., 2014; 2017; Jackson et al., 2017; Hogan et al., 2016; Sheldon et al., 2016), and we note that prior to 2011, many publications used a  $\Delta R=0$  years (Andrews et al., 1998; Knudsen et al., 2008). However, recognizing that the marine reservoir offset could be large and variable over the time interval of 12PC and because this core extends into the LGM, defined here as beginning at 26.5 ka (Clark et al., 2009) and ending at the beginning of the Oldest Dryas period, 18 ka BP (Buizert et al., 2014), we used the variable North Atlantic R values in Stern and Lisiecki (2013) to provide an envelope of calibrated age so that we could consider the correlations of boundaries and conditions recorded in the core with established climatic intervals (Fig. 3f). To accomplish this we first calibrated each date with  $\Delta R=0.14$ C years, which provides the maximum age. We then used the  $\Delta R=0$  ages to identify the appropriate 500 year bin of maximum, average and minimum R values from Table S1 of Stern and Lisiecki (2013) and calibrated each of the dates using these three R-values. The resulting envelope of ages, from  $\Delta R=0$  to the maximum Stern and Lisiecki 2013 R-value, illustrates how the choice of  $\Delta R$  affects correlation of boundaries in the core with climate intervals from LGM through the YD (Fig. 3f; Table 1). Regardless, these results confirm that the core contains LGM and Heinrich Stadial 1 (aka Oldest Dryas) sediments, a key requirement for testing the ice shelf model (Hulbe et al., 1997; Álvarez-Solas et al., 2010; Marcott et al., 2011).

3.2 Foraminiferal analyses.

One-cm wide samples were weighed wet and sieved on a 63-µm screen. Material >63 µm was kept wet in a storage solution of 70% distilled water and 30% ethanol with baking soda as a buffer. Foraminifera were counted wet to prevent destruction of fragile tests that disintegrate under the stress of drying. A wet splitter was used when necessary to achieve a count of 200-300 benthic formaminifers and as many planktic foraminifers as were in the benthic split. In most cases the full sample was counted. Equivalent dry weights of the foram samples were estimated from sedimentology samples from the same depths that had both wet and dry weights, allowing foraminifera/gram sediment to be calculated.

# 3.3 Stable isotope analyses

Stable oxygen and carbon isotopes were measured on the planktic foram species  $Neogloboquadrina\ pachyderma\$ picked from the 150-250  $\mu$ m size fraction in 41 samples; results from 3 samples were rejected because they yielded a low signal. Samples >100  $\mu$ g have standard deviations of 0.01 and 0.03 % for  $\delta^{13}$ C and  $\delta^{18}$ O respectively. Samples weighing <100  $\mu$ g are reported with a standard deviation of 0.06 % for  $\delta^{13}$ C, and an error of  $\pm 0.2$  % for  $\delta^{18}$ O. The oxygen isotope values are expressed as % vs VPDB. Between 1050 and 857 cm all samples were of small weight but otherwise seemed reliable. Measurements were made on a Micromass IsoprimeTM dual inlet coupled to a MulticarbTM system at the Light Stable Isotope Geochemistry Laboratory at the University of Montréal – UQAM.

3.4 CT scan.

216

217

218

219

220

221

222

223

224

225

226

227

228

229

230

231

232

233

234

235

236

237

238

CT scanning of the half round core was performed at the sediment core laboratory at the University of Quebec at Rimouski. A CT number (a measure of sediment density) was extracted from the images. The CT scan image was used to determine lithofacies and boundaries, sedimentary structures, and to identify bioturbation, a key source of evidence for the presence of benthic organisms and a source of information about sedimentation rate variations between the radiocarbon dates (Wetzel, 1991). Counts of >2 mm clasts interpreted as ice rafted detritus (IRD) were made from the CT images by counting in a 2 cm wide window across the core width continuously along the core length (Grobe, 1987). 3.5 Biomarkers: IP<sub>25</sub> and Brassicasterol Biomarker analyses (IP<sub>25</sub> and brassicasterol) were performed using methods described previously (Belt et al., 2012; Belt et al., 2015). Briefly, 9-octylheptadec-8-ene (9-OHD, 10 μL; 10 μg mL<sup>-1</sup>) and  $5\alpha$ -androstan-3β-ol (10 μL; 10 μg mL<sup>-1</sup>) were added to ca. 1-2g of each freeze-dried sediment sample prior to extraction to permit quantification of IP<sub>25</sub> and sterols, respectively. Samples were then extracted using dichloromethane/methanol (3 x 3 mL; 2:1 v/v) and ultrasonication. Following removal of the solvent from the combined extracts using nitrogen, the resulting total organic extracts (TOE) were purified using column chromatography (silica) with IP<sub>25</sub> (hexane; 6 mL) and brassicasterol (20:80 methylacetate/hexane; 6 mL) collected as two single fractions. Non-polar lipid fractions

Saturated hydrocarbons were eluted with hexane (1 mL), while unsaturated hydrocarbons

were further separated into saturated and unsaturated hydrocarbons using glass pipettes

containing silver ion solid phase extraction material (Supelco Discovery® Ag-Ion).

(including IP<sub>25</sub>) were eluted with acetone (2 mL). All fractions were dried under a stream of nitrogen.

Analysis of individual fractions was carried out using gas chromatography - mass spectrometry (GC-MS) with operating conditions as described previously (e.g. Belt et al., 2012; Brown and Belt, 2012). Sterols were derivatized (BSTFA; 50  $\mu$ L; 70 °C; 1 h) prior to analysis by GC-MS. Mass spectrometric analysis was carried out in total ion current (TIC) and single-ion monitoring (SIM) modes. Individual lipids were identified on the basis of their characteristic GC retention indices and mass spectra obtained from standards. Quantification of IP<sub>25</sub> was achieved by dividing its integrated GC-MS peak area by that of the internal standard (9-OHD) in SIM mode (both m/z 350) and normalizing this ratio using an instrumental response factor (obtained from laboratory standards of each analyte) and the mass of sediment (Belt et al., 2012). Analytical reproducibility (6 %, n = 3) was monitored using a sediment with a known concentration of IP<sub>25</sub>. Brassicasterol concentrations were obtained by comparison of their respective peak areas in SIM mode (brassicasterol, m/z 470) with those of the internal standard (m/z 333) and normalized as per IP<sub>25</sub>.

3.6 Quantitative X-ray diffraction Mineralogy

Quantitative x-ray diffraction (qXRD) analyses were used to identify shifts in sediment sources between 'local' West Greenland (WG) and 'distal' Northern Baffin Bay (NBB). Samples for qXRD analysis were taken at 10 to 20 cm intervals throughout the core. Sediment samples were freeze-dried and processed at INSTAAR using the method described by Eberl (2003) and Andrews and Eberl (2011). The qXRD samples were

analysed on a Siemens D5000 XRD unit at a 0.02 2-0 step with a 2 second count; minerals were identified using the program RockJock v.6 (Eberl, 2003). The qXRD 2-source data to 17.5 cal ka BP is presented in Jennings et al. (2017). The determination of sediment provenance is based on the quantitative X-ray diffraction (qXRD) analysis of the < 2 mm surface and core sediments using the method outlined by Eberl (2003) and described in more detail for our area by (Andrews and Eberl, 2012; Andrews et al., 2014; O'Cofaigh et al., 2013a; Simon et al., 2014). We use the Excel macro unmixing program "SedUnMix" (Eberl, 2004; Andrews and Eberl, 2012) to ascribe sediment mineral assemblages to probable source areas. In this present study we discriminated between two glacial derived sources; first a regional West Greenland source dominated by specific ranges in quartz, plagioclase, k-feldspars and other non-clay and clay minerals, versus a North Baffin Bay detrital carbonate source dominated by dolomite (Andrews et al., 2014; O'Cofaigh et al., 2013; Jennings et al., 2017).

# 4. Results and Interpretation

#### 4.1 Lithofacies Characteristics

There are two main lithofacies units defined by the sediment parameters in 12PC (Fig. 3). The boundary between the two units (Fig. 4b) is well expressed by an abrupt shift to lower CT# (Fig. 3A). This transition dates to 16.2 cal ka BP using  $\Delta R$ =140 years and has been interpreted to represent the retreat of the Greenland Ice Sheet from the shelf edge (Jennings et al., 2017). However, the full age-envelope ranges between 16.4 ( $\Delta R$ =0) to 14.0 (Max R) ka, or, late in Heinrich Stadial 1 to the end of the Bølling (Fig. 3f). Calibrated radiocarbon dates (Fig. 3F;  $\Delta R$ =140, pink) in the lower unit range from

21.8 to 16.2 cal ka BP. The lower three radiocarbon dates fall within the LGM regardless of the marine reservoir age selected (Fig. 3F). The radiocarbon date at 571.5 cm falls within Heinrich Stadial 1 regardless of the marine reservoir age (Fig. 3F).

The lower lithofacies unit, which represents the period when the ice sheet grounding line was at or near the shelf edge, has higher magnetic susceptibility (Fig. 3C), variable sand content including high weight percentage peaks (Fig. 3D) and a west Greenlandic sediment composition (Fig. 3E) but rare >2mm clasts (Fig. 3B). From the base of the core to 1022 cm, sediments are laminated mud with straight, sharp contacts defining the laminae and vertically oriented burrows (Fig. 4f). Between 1025 and 768 cm the sand content increases and stratification is disrupted by bioturbation (Fig. 3E). Stratified mud with distinct vertical burrows extends from 768 to 735 cm (Fig. 3D). From 735 cm to 688 cm sand content increases. This sandy unit is overlain by another sequence of stratified mud with distinct burrows between 688 and 630 cm. The sediment between 630 and 467 cm is bioturbated, stratified mud with layering disturbed by bioturbation (Fig. 4c). The uppermost part of this unit has high sand content and marks the transition to the upper lithofacies unit.

The upper lithofacies from 467 to 0 cm, which represents deglaciation and the Holocene (Jennings et al., 2017), has overall lower CT number (lower density) (Fig. 3A), lower magnetic susceptibility (Fig. 3C) and generally lower sand content (Fig. 3D). But, it has much higher numbers of >2mm clasts (IRD) (Fig. 3B). Immediately above the boundary the sediments are low-density bioturbated mud with the sand fraction comprising *Coscinodiscus* planktic diatoms and setae of *Chaetoceras*, consistent with the low MS values (Fig. 3c). Well-defined, thin laminae and rare IRD occur at the base of the

unit, but transition upward to less-well defined laminae and rare to absent IRD from 420 cm to 352 cm. This fine interval was interpreted to record a period in the initial deglaciation as the grounding line retreated off the shelf edge with retention of an ice shelf (Jennings et al., 2017). At 352 cm (marked by middle horizontal blue line on Figure 3) the CT # (density), MS and sand increase (Fig. 3A, B, C, D). This level marks the start of renewed retreat of the GIS grounding line by calving (Jennings et al., 2017). The sediments are bioturbated but stratification is still evident, suggesting moderate sedimentation rates. Apart from a peak in >2mm clasts of west Greenland provenance at 330 cm the main rise in >2mm clasts coincides with the entry of the Northern Baffin Bay sediment source (NBB source) at 290 cm (Fig. 3B, E). Bioturbated, pebbly mud associated with a rise in NBB provenance occurs between 280 and 175 cm with the highest IRD interval from 280-240 cm (Fig. 3B, E). This NBB DC interval has been found in several cores on the central West Greenland slope (Sheldon et al., 2016; Jennings et al., 2017; Jackson et al., 2017) and has been correlated to BBDC1 (Simon et al., 2012; 2014; Jackson et al., 2017), marking the retreat of NBB ice streams. The NBB DC event is overlain by bioturbated mud with small, dispersed IRD and discontinuous silt stringers between 175 and 152 cm. Bioturbated pebbly mud between 152 and 52 cm has high NBB provenance between 160 and 90 cm, an interval that contains an age reversal and a mixture of radiocarbon ages (Fig. 3F). The age reversal suggests that the upper NBB peak is reworked. The upper 52 cm of the core is bioturbated mud with dispersed IRD likely represents the middle to late Holocene time period, although it is undated.

329

330

308

309

310

311

312

313

314

315

316

317

318

319

320

321

322

323

324

325

326

327

328

4.2 Biological Proxies

Biological proxy data are expressed against age using the age model based on  $\Delta R$ =140 yrs (Fig. 5).

#### 4.2.1 Bioturbation

333

334

335

336

337

338

339

340

341

342

343

344

345

346

347

348

349

350

351

352

353

The CT scan image (Fig. 3) reveals that the entire core is bioturbated, indicating that there was sufficient oxygenation and food to support the benthos in Baffin Bay throughout the time period represented by the core (Löwemark et al., 2012). Variations in burrow shape and density are indicative of the interplay between oxygenation, sedimentation rate, sedimentation processes, substrate consistency and food supply (Reineck and Singh, 1980, Wetzel, 1991; Löwenmark et al., 2012) (Fig. 4). Intensely bioturbated intervals in which sand layers are disrupted by burrowing (e.g. Fig. 4a, c, e) suggest periods of relatively slow sedimentation (Wetzel, 1991), whereas intervals of vertical burrows terminated by overlying strata (e.g. Fig. 4d, f) indicate episodic rapid sedimentation (Jennings et al., 2011a). Figure 4 shows expanded views of segments of the CT image shown in full on Figure 3 to illustrate some of the key lithofacies characteristics and trace fossil types that provide evidence for sedimentation processes. Muddy intervals typically have vertical burrows that are truncated by subsequent strata (Fig. 4d). These mud intervals likely represent plumites deposited from turbid meltwater plumes, whereas the sandy, stratified intervals with varying degrees of bioturbation likely represent distal turbidites (Ó Cofaigh and Dowdeswell, 2001) (Fig. 4c, f). 4.2.2 Foraminifera and Stable Isotopes The Foraminiferal abundances in 12PC are spiky, with intervals of low benthic and planktic numbers per gram of dry sediment punctuated by periods of much higher

numbers of foraminifers per gram (Fig. 5D). The high variability in abundance relates to

variations in marine productivity, overprinted by carbonate dissolution, and dilution by high (12.8 cm/ka on average from 250-860 cm) and varying sedimentation rates. The lithofacies characteristics suggest widely varying sedimentation rates in the core that are not captured by the less frequent age control. Therefore we did not attempt to calculate foraminiferal flux, which would have been a more direct measure of productivity, but rather rely on foraminiferal numbers per gram as a measure of productivity.

N. pachyderma, the only planktic species, forms abundance spikes up to 1620 specimens/g, with intervening periods of very low abundance to absence (Fig. 5). The planktic forams were quite small from the base of the core to 860 cm (22 cal ka BP), but increased in size above that level. In general the planktic and benthic foram abundances rise and fall together, suggesting that the abundance spikes represent in situ productivity and a link between surface productivity and benthic food supply, although we cannot control for variations in carbonate preservation. Low numbers of N. pachyderma per gram are consistent with low productivity under perennial sea ice and the high numbers per gram are consistent with periods of more open water, such as leads or polynyas in summer (e.g. Nørgaard-Pedersen et al., 2003). Advection of planktic foraminifers from outside Baffin Bay is unlikely, especially given the linkage between the benthic and planktic productivity (cf Knutz et al., 2011; Nørgaard-Pedersen et al., 2003).

Oxygen isotope values on *N. pachyderma* ranged between 5.4 and 2 ‰. The interval between 22 and 18.2 cal ka BP has mostly heavy values that fall between 4 and 5 ‰ (Fig. 5), comparable to MIS 2 values in the Fram Strait (Nørgaard-Pedersen et al., 2003). A shift to lighter  $\delta^{18}$ O and  $\delta^{13}$ C values begins at 18 cal ka BP, suggests reduced ventilation (Sarnthein et al., 1995). This interval falls within HS1 regardless of which  $\Delta$ R

is applied (Fig. 2; Table 1). Above this shift the  $\delta^{18}$ O values remain above 3.7 ‰. A pronounced light  $\delta^{18}$ O spike at 19.4 cal ka BP corresponds to high planktic abundance and increased IP<sub>25</sub> and Brassicasterol (Fig. 5). Oxygen isotopic values of this magnitude can either be related to glacial meltwater, especially if they are paired with light  $\delta^{13}$ C values (Sarnthein et al., 1995) or to increased rate of sea-ice production that can produce brines with a light isotopic signature (Hillaire-Marcel et al., 2004; Hillaire-Marcel and de Vernal, 2008). The overall trend in the  $\delta^{13}$ C values is toward heavier values suggesting better ventilation at the top of the record than at the bottom (Fig. 5).

377

378

379

380

381

382

383

384

385

386

387

388

389

390

391

392

393

394

395

396

397

398

399

The benthic foraminiferal assemblages (Fig. 6) provide insights into the productivity of surface waters, stratification of the water column, and turbid glacial meltwater influx. For example, sea-ice edge migration, either seasonal or in the form of leads or polynyas, produces pulses of phytoplankton production that sink to the seabed, providing food for benthic communities. The three most common benthic foraminiferal species in 12PC are Stainforthia feylingi, Cassidulina reniforme and Elphidium excavatum forma clavata. S. feylingi is dominant in conditions of stratified water column with a cold freshwater lid and has been associated with productivity at the seasonal sea ice edge (Seidenkrantz, 2013). It has been found in high abundances associated with biosiliceous sediments (Jennings et al., 2006). E. excavatum and C. reniforme occur together in glacial marine settings (Hald and Korsun, 1997). C. reniforme is also considered to represent chilled Atlantic Water (Slubowska et al., 2005) and is found in areas of relatively high, stable salinities (Polyak et al., 2002). E. excavatum is an opportunistic species that thrives in unstable environmental conditions influenced by rapid sedimentation and fluctuating salinities from turbid meltwater plumes (Hald and

Korsun, 1997). The agglutinated species, *Spiroplectammina biformis*, which occurs mainly in the lower lithofacies unit is found in arctic fjords with strong meltwater signal (Jennings and Helgadottir, 1994; Schaffer and Cole, 1986).

Several species indicative of marine productivity associated with nutrient rich Atlantic Water occur in both the lower and upper lithofacies unit: *Melonis barleeanus*, *Buccella frigida*, *Nonionella turgida* and *Nonionellina labradorica*. *Islandiella norcrossi* and *I. helenae* both are arctic species, but *I. helenae* is associated with sea-ice edge productivity while *I. norcrossi* reflects chilled Atlantic Water of normal marine salinity (Polyak et al., 2002; Wollenburg et al., 2004; Lloyd, 2006). *I. norcrossi* is a common calcareous species on the west Greenland shelf associated with Atlantic Water in the West Greenland Current (e.g. Lloyd, 2006; Perner et al., 2012).

Near the top of the lower unit (16.5 cal ka BP), and continuing into the base of the overlying biosiliceous mud, several species associated with marine productivity and nutrient rich Atlantic Water spike to high percentages. These include *N. turgida*, *M. barleeanus*, *B. frigida*, *I. norcrossi* and very low percentage of *Pullenia bulloides*.

Current indicator species, *Cibicides lobatulus* also increases at this boundary. The central part of the diatom-rich mud is barren of calcareous foraminifers and is characterized by low faunal abundances dominated by agglutinated foraminiferal species (e.g. *Textularia earlandi*), suggesting that dissolution of carbonate likely overprinted the assemblages.

The upper part of the diatom-rich mud shows a return of several of the marine productivity species along with increased percentages of *P. bulloides*, a chilled Atlantic water species, that is common on the SE Greenland and Northern Iceland shelves under

conditions of strong Irminger Current Atlantic water inflow (Eiríksson et al., 2000; Jennings et al., 2011b).

Above the diatom-rich mud, the percentages of *N. labradorica* and *I. norcrossi* increase, and *S. feylingi* continues with high percentages. The chilled Atlantic Water species, *Cassidulina neoteretis*, is abundant at the top of the dated section along with *I. norcrossi*, consistent with intermediate Atlantic Water and less prominent glacial meltwater influence (Jennings and Helgadottir, 1993). The gap in foraminifers between 12 and 13.9 cal ka BP is likely a consequence of carbonate dissolution as other cores from the central West Greenland margin, but in slightly shallower water (JR175-VC29; Fig. 1) have *C. neoteretis* continuously between 14 and 11 cal ka BP (Jennings et al., 2017).

# *4.2.3 Biomarkers*

Further evidence of marine productivity and sea ice comes from the algal biomarkers brassicasterol and IP<sub>25</sub> (Fig. 5). In general, the presence of IP<sub>25</sub> indicates release from melting seasonal sea ice (Fahl and Stein, 2012; Belt et al., 2013), while the absence of IP<sub>25</sub> is consistent with intervals of thick perennial sea ice cover or no ice cover at all (Fahl and Stein, 2012). Brassicasterol implies productivity in open-water conditions, but it also can come from melting sea ice (Belt et al., 2013). In addition, the occurrence of polynyas has been given as a possible reason for presence of IP<sub>25</sub> and brassicasterol under otherwise heavy ice conditions, even in the central Arctic Ocean (Xiao et al., 2013). In the lower, high CT lithofacies unit of 12PC, brassicasterol and IP<sub>25</sub> are present in low abundances from 26 to 22 ka ( $\Delta$ R=140 yrs), coinciding with low foraminiferal

abundances (Fig. 5). Between 22 and 20 ka, brassicasterol rises but  ${\rm IP}_{25}$  is low to absent.

Foraminiferal abundances rise in this interval and the benthic fauna is characterized by productivity species (*B. frigida*, *I. helenae*, *M. barleeanus* and *N. labradorica*). An overall rise in IP<sub>25</sub> and a large peak in brassicasterol occur at 19.5 ka, and continue with moderate values until another rise in brassicasterol values within the diatom-rich mud unit (16.2 to 15.1 cal ka BP). Both IP<sub>25</sub> and brassicasterol continue to rise after 15.1 cal ka BP, but IP<sub>25</sub> in particular rises to values unprecedented in the core after 14.3 cal ka BP.

This pattern of presence of  $IP_{25}$  and brassicasterol in the lower lithofacies unit argues for seasonal sea ice and some open water, although the generally low concentrations suggest that these were both likely less than in the upper unit - probably due to more extensive ice cover and only periodic opening - possibly as leads or polynyas. As the final increase in  $IP_{25}$  beginning at 16.2 ka is accompanied by rising, high brassicasterol it likely points to development of a marginal ice zone where there is increased marine productivity with probably more seasonal sea ice presence than before.

#### 5. Discussion

5.1 Did an LGM Ice Shelf cover Baffin Bay?

There has been limited research on the LGM within Baffin Bay, which explains how the Baffin Bay ice shelf concept has remained untested. Radiocarbon dates on planktic foraminifers indicate that other cores besides 12PC have planktic fauna in the LGM. Andrews et al (1998) obtained a pair of AMS  $^{14}$ C dates from abundant planktic foraminifera in southern Baffin Bay core HU77029-017PC (17,990 ± 110, and 17,930 ± 210  $^{14}$ C yrs; Andrews et al., 1998) (Fig. 1). These  $^{14}$ C ages calibrate to the LGM (~21 ka BP;  $\Delta$ R=140 years). A  $^{14}$ C date on planktic foraminifers from core HE006-4-2PC

 $(21,440\pm 140^{14}\text{C yrs})$  on the northern side of the Uummannaq TMF (Fig. 1) calibrates to ~25 ka BP ( $\Delta$ R=140 years) (Ó Cofaigh et al., 2013a). In the LGM interval of 12PC (1130 cm to at least 690 cm) when the modeled Baffin Bay ice shelf would be in place, there are multiple lines of evidence for biological activity, including bioturbation, algal biomarkers and benthic and planktic foraminifers (Figs. 3 - 6). These findings are consistent with perennial sea-ice cover with some open water in the form of leads or polynyas on the eastern side of Baffin Bay. Full ice-shelf cover from an ice shelf extending from the Hudson Strait ice stream and grounding on Davis Strait all the way to Greenland (Alvarez-Solas et al., 2010; 2011; Marcott et al., 2011) would not allow the surface productivity (e.g. algal biomarkers, planktic forams) in Baffin Bay that would be needed to feed the benthic organisms that are evident (bioturbation and benthic foraminifers). On this basis we reject the modeling result of a full Baffin Bay ice shelf. While life has been observed under modern ice shelves in Antarctica, it is dependent on strong ocean inflow to the sub ice-shelf cavity from outside the ice shelf (Post et al., 2014). In the case of the Baffin Bay ice shelf cover as it is modeled, it would be sealed from the Labrador Sea marine advection and food supply. The idea of the Davis Strait grounded ice shelf sprang in part from efforts to test a mechanism for Heinrich Event 1 (H1), in which subsurface warming reconstructed in the N. Atlantic in response to reduced Atlantic meridional overturning circulation (AMOC) during HS1 (McManus et al., 2004) weakens a buttressing ice shelf fronting the Hudson Strait ice stream and produces a Heinrich event (Álvarez-Solas et al., 2010; 2011; Marcott et al., 2011). Hulbe et al. (2004) modified their original 1997 Labrador Sea ice shelf idea to support instead fringing ice shelves along the coasts in Eastern Canada that

468

469

470

471

472

473

474

475

476

477

478

479

480

481

482

483

484

485

486

487

488

489

were proposed to have met their demise through a process of meltwater infilling of surface crevasses. The existence of this type of ice shelf and H-event process has been contested (Alley et al., 2005), but it is more consistent with the 12PC data than the original idea of an ice shelf grounding on Davis Strait (Hulbe et al., 1997).

#### 5.2 Heinrich Stadial Environments

491

492

493

494

495

496

497

498

499

500

501

502

503

504

505

506

507

508

509

510

511

512

513

The data in 12PC allow examination of the environmental response in Baffin Bay to the transition from LGM to HS1, and the response in Baffin Bay to the large ice discharge from Hudson Strait during H1 which occurred when subsurface ocean heat was at a maximum and AMOC at a minimum (Marcott et al., 2011). Locating the LGM/HS1 transition and H1 in 12PC is made difficult by the uncertainties in the magnitude of the local marine reservoir age through time (Fig. 3F) (Stern and Lisiecki, 2013). The accepted timing of H1 calving event is 16.8 ka BP (Hemming, 2004), although it may be closer to 16 ka BP based on the timing of the peak of IRD in the North Atlantic IRD stack during HS1 (Stern and Lisiecki, 2013). If we apply the  $\Delta R$  envelope approach using data from Stern and Lisiecki (2013) to the mean value of the best 2 constraining radiocarbon ages from the base of DC1 (=H1) in cores HU75009-IV-055PC and HU87033-009 LCF (Fig. 1; Andrews et al., 1994; Jennings et al., 1996), from the Labrador Sea, we obtain a range of ages for the event that spans HS1 (Table 1). The  $\Delta R$ that matches best the H1 16.8 ka age determined by Hemming (2004) is the lower  $\Delta R$ from Stern and Lisiecki (2013) (Table 1). On this basis, we chose to use the Lower  $\Delta R$  to determine where HS1 lies in the 12PC record. Lower ΔR places the base of HS1 (18 ka BP) at 610 cm and its end (14.7 ka BP) at 395cm, right at the end of the diatom-rich mud unit and before the initiation of calving retreat (Fig. 3F and 7). Lower  $\Delta R$  also puts the

calving retreat and the timing of the west Greenland DC event (=BBDC1; Jackson et al., 2017) (Fig. 3) in the Bølling/Allerød interstadial (Fig. 7). The age model calculated with an invariant  $\Delta R$ =140 years places the lithofacies transition which represents the grounding line retreat from the west Greenland shelf edge at 16.2 cal ka BP, within HS1 (Jennings et al., 2017), but places the end of HS1 after the initiation of GIS calving retreat.

Figure 7 illustrates how key proxy data map into the Heinrich Stadial interval defined by evidence of sluggish AMOC (McManus et al., 2004) using the lower  $\Delta R$  of Stern and Lisiecki (2013). In the Labrador Sea HS1 is an interval of anomalously warm bottom waters (Marcott et al., 2011) within which H1 occurred (Fig. 7). We would expect this massive freshwater (meltwater and icebergs) outflow from collapse of the Hudson Strait ice stream (Andrews and Tedesco, 1992; Hesse and Khodabakhsh, 2016) to perturb environments in Baffin Bay or initiate a transition to different paleoceanographic conditions.

The transition to lighter  $\delta^{18}$ O values and a shift to very high percentages of *S. feylingi* coincide with HS1 (Fig. 7). This signal is also seen in nearby core JR175-VC29 (Fig. 1), from 900 m water depth (Jennings et al., 2017) and is associated in both 12PC and VC29 with deposition of diatom-rich mud with rare IRD; a fine-grained unit of similar age is observed in core GeoTü SL-170 (Jackson et al., 2017) slightly north of VC29. The diatom-rich mud interval has been interpreted by Jennings et al. (2017) to indicate exclusion of coarse sediment delivery to the Disko TMF by retention of a fringing ice shelf after initial grounding line retreat. Overall, brassicasterol abundances are low in HS1. A period of high productivity of benthic forams indicative of nutrient

rich Atlantic water at the subsurface (Fig. 5) (indicated on Fig. 7 by red stars and low percentages of the benthic foraminiferal species, *S. feylingi* ) coincides with the initial GIS retreat from the shelf edge as indicated in the CT# profile (Jennings et al., 2017). Subsequent interstadial conditions are marked by rising marine productivity, renewed subsurface Atlantic Water influence, and renewed retreat of the GIS, followed by development of consistent seasonal sea ice and release/melting of detrital carbonate bearing ice bergs from ice margins of northern Baffin Bay termed a west Greenland DC event by (Jennings et al., 2017) that has been shown to be correlative to BBDC1 (Simon et al. (2016) by Jackson et al. (2017).

#### 6. Conclusions

1. Based on the data presented we reject the hypothesis that Baffin Bay was covered by a full ice shelf during the LGM. We conclude instead that Baffin Bay was perennially seaice covered with nutrient rich, relatively warm Atlantic water present at depth through the LGM. Evidence of marine productivity suggests that there were openings in the sea-ice cover as leads and polynyas to support marine productivity. Concurrently, sediment-laden, glacial-meltwater and turbidity currents were released from the GIS, grounded at the shelf edge, but IRD was rare suggesting the ice front was protected by a fringing ice shelf and/or the perennial sea-ice cover.

2. Reduced ventilation and productivity, coincident with a cold surface lid of meltwater was established in HS1. After Heinrich Event 1, but within the Heinrich stadial, an interval of increased productivity and Atlantic Water is associated with the retreat of the GIS grounding line from the shelf edge.

560 3. The implication for Heinrich Events and Ocean warming/Ice Shelf hypothesis is that 561 perennial sea-ice cover and/or fringing ice shelves may be sufficient to explain the heat 562 retention and back-pressure proposed to explain the dynamics that produce Heinrich 563 Events. 564 565 7. Acknowledgements 566 Funding for this research was provided by the US National Science Foundation grant 567 ARC1203492 and the UK Natural Environment Research Council grant NE/D001951/1. 568 We thank the captain, crew and scientists aboard the 2008 CSS Hudson cruise HU2008-569 029 for acquisition of core 2009029-12PC. We gratefully acknowledge the microscope 570 and x-ray diffraction research by undergraduate research assistants, Brian Shreve, 571 Jennifer Kelly, Matthew Reed, and Matthew Glasset. We thank Quentin Simon and one 572 anonymous reviewer for helpful critique of the manuscript. 573 574 8. Figure Captions 575 Figure 1. Bathymetric map centered on Baffin Bay (BB) showing the location of core 576 HU2008029-12PC (12PC) and other cores mentioned in the text, the distribution of 577 Paleozoic carbonate bedrock, mapped ice margin positions in northern Baffin Bay (Li et 578 al., 2011) and central west Greenland (Ó Cofaigh et al., 2013a) and major ice streams. 579 UIS = Uummannaq ice stream; DIS = Disko ice stream; SSIS = Smith Sound ice stream; 580 LSIS = Lancaster Sound ice stream. Northward flowing West Greenland Current (WGC) 581 is shown as the thin red line and the southward flowing Baffin Current (BC) is shown as

a thin blue line. The position of the acoustic profile in Figure 2 is shown as a black line.

583 HU2008029-016PC=16; HE006-4-2PC=2; JR175-VC29=29; HU77029-017PC=17; 584 HU75009-IV-055PC=55 and HU87033-009 LCF=9. Inset plot shows the salinity and 585 temperature against water depth at from the same location as 2008029-12PC. 586 ASW=Arctic Surface Water; WGIW=West Greenland Intermediate Water; DBBW=Deep 587 Baffin Bay Water. 588 589 Figure 2. A. 3.5 kHz sub-bottom profile over the site of 2008029-12PC demonstrationg 590 the acoustically-stratified character of the seabed in the area. B. A zoom in map of the 3.5 591 kKz sub-bottom profile and the core location shown in Figure 1. The bathymetry is from 592 GEBCO. 593 594 Figure 3. Lithological proxies and age control for 2008029-12PC. A is the CT image 595 against depth in the core. Black bars along depth axis show the locations of CT images 596 shown in Figure 4. 'V' denotes locations of vertical burrows. B. IRD counts (>2mm 597 clasts) from CT scan in 2 cm increments. C. CT number, a measure of density derived 598 from the CT image. D. Magnetic Susceptibility measure by multi sensor track (MST). E. 599 Weight percentage of >63 µm sand fraction from foraminiferal samples. F. Two-source 600 provenance of minerals: Northern Baffin Bay (NBB, brown) vs. the local source, central 601 west Greenland (green). F. Depth-Age model in pink ( $\Delta R=140\pm30$  yrs) showing  $1\sigma$  and 602  $2 \sigma$  uncertainties of the model. Excluded from the model are benthic foraminiferal ages 603 (green distributions) and outliers at 1 meter. Age envelope for other potential  $\Delta R$ 604 calibrations are shown by blue ( $\Delta R=0$ ); Red, green, orange = lower, mean, and upper  $\Delta R$ 605 values from Stern and Lisiecki (2013). Climate units are along the age scale.

606	
607	Figure 4. Examples of lithofacies and bioturbation types from 2008029-12PC CT scans.
608	See Figure 3 for locations of these examples on the CT image of the core.
609	
610	Figure 5. Biological proxies from 12PC compared with CT# plot to assist with
611	comparison to depth on depth in Figure 3. A. CT#; B. sea ice biomarker, IP <sub>25</sub> ; C. marine
612	productivity biomarker, brassicasterol; D. Benthic (blue) and planktic (red) forams per
613	gram of dry sediment; E. $\delta^{18}$ O of planktic foraminifer, <i>N. pachyderma</i> , blue; F. $\delta^{13}$ C of <i>N</i> .
614	pachyderma, green.
615	Figure 6. Benthic foraminiferal species in 12PC. Green represent marine productivity
616	species; Red=Atlantic Water species; Blue = Arctic species; Light Blue; Glacial marine
617	species; Orange=transformed (cooler and slightly lower salinity) Atlantic Water species.
618	
619	Figure 7. Comparison between Pa/Th record of AMOC (McManus et al., 2004) and the
620	timing of Heinrich Event 1 (H1) to key paleoenvironmental proxies in 12PC. The HS1
621	interval (yellow box) is defined in the core with use of the Lower $\Delta R$ of Stern and
622	Lisiecki (2013) (Fig. 3f). Blue lines show where key events in the core map into the
623	climatic intervals with use of the Lower $\Delta R$ of Stern and Lisiecki (2013). A. CT # from
624	12PC; B. Brassicasterol, 12PC; C. IP <sub>25</sub> , 12PC; D. Stainforthia feylingi, 12PC; E. Oxygen
625	isotope ratios, 12PC; F. Pa/Th ratios (McManus et al., 2004).
626	
627 628 629 630 631	Aksu, A. E., 1985. Climatic and oceanographic changes over the past 400,000 years: Evidence from deep-sea cores on Baffin Bay and David Strait. <i>In</i> Andrews, J. T. (ed.), <i>Quaternary Environments: Eastern Canadian Arctic, Baffin Bay and Western</i>

- Alley, R. B., Andrews, J. T., Barber, D. C., and Clark, P. U., 2005: Comment on
- "Catastrophic ice shelf breakup as the source of Heinrich event icebergs" by C.L.
- 635 Hulbe et al. *Palaeoceanography*, 20: doi:10:1029/2004PA001086.

636

- 637 Álvarez-Solas, J., Charbit, S., Ritz, C., Paillard, D., Ramstein, G., and Dumas, C.: Links
- 638 between ocean temperature and icebergdischarge during Heinrich events, *Nature*
- 639 *Geoscience*, 3, 122–126, 2010

640

- Álvarez-Solas, J., Montoya, M., Ritz, C., Ramstein, G., Charbit, S., Dumas, C.,
- Nisancioglu, K., Dokken, T., Ganopolski, A., 2011. Heinrich event 1: an example of
- dynamical ice-sheet reaction to ocean changes. *Climate of the Past* 7, 1297-1306.
- 644 doi:10.5194/cp-7-1297-2011.

645

- Andrews, J.T., Eberl, D.D., 2011. Surface (sea floor) and near-surface (box cores)
- sediment mineralogy in Baffin Bay as a key to sediment provenance and ice sheet
- 648 variations. *Can. J. Earth Sci.* 48 (9), 1307 1328. http://dx.doi.org/10.1139/-11-021.

649

- Andrews, J.T., Eberl, D.D., 2012. Determination of sediment provenance by unmixing
- the mineralogy of source-area sediments: The "SedUnMix" program. *Marine Geology*
- 652 291, 24-33.

653

- Andrews, J.T., Erlenkeuser, H., Tedesco, K., Aksu, A., Jull, A.J.T., 1994. Late Quaternary
- 655 (Stage 2 and 3) Meltwater and Heinrich events, NW Labrador Sea. *Quaternary*
- 656 Research 41, 26-34.

657

- Andrews, J.T. Gibb, O.T., Jennings, A.E., Simon, Q., 2014. Variations in the provenance
- of sediment from ice sheets surrounding Baffin Bay during MIS 2 and 3 and export
- to the Labrador Shelf Sea: site HU2008029-0008 Davis Strait. *Journal of Quaternary*
- 661 *Science* 29, 3-13.

662

- Andrews, J. T., Kirby, M. E., Aksu, A., Barber, D. C., and Meese, D., 1998. Late
- Ouaternary Detrital Carbonate (DC-) events in Baffin Bay (67° 74° N): Do they
- correlate with and contribute to Heinrich Events in the North Atlantic? *Quaternary*
- 666 *Science Reviews,* 17: 1125-1137.

667

- Andrews, J. T. and Tedesco, K., 1992: Detrital carbonate-rich sediments,
- 669 northwestern Labrador Sea: Implications for ice-sheet dynamics and iceberg rafting
- 670 (Heinrich) events in the North Atlantic. *Geology*, 20: 1087-1090.

671

- Belt, S.T., Brown, T.A., Navarro Rodriguez, A., Cabedo Sanz, P., Tonkin, A., Ingle, R.,
- 673 2012. A reproducible method for the extraction, identification and quantification of
- the Arctic sea ice proxy IP25 from marine sediments. *Analytical Methods* 4, 705-713.

- Belt, S.T., Brown, T.A., Ringrose, A.E., Cabedo-Sanz, P., Mundy, C.J., Gosselin, M.,
- 677 Poulin, M., 2013. Quantitative measurement of the sea ice diatom biomarker IP25

- and sterols in Arctic sea ice and underlying sediments: Further considerations for
- palaeo sea ice reconstrucion. *Organic Geochemistry* 62, 33–45.

- Belt, S.T., Cabedo-Sanz, P., Smik, L., Navarro-Rodriguez, A., Berben, S.M., Knies, J.,
- Husum, K., 2015. Identification of paleo Arctic winter sea ice limits and the marginal
- 683 ice zone: Optimised biomarker-based reconstructions of late Quaternary Arctic sea
- ice. *Earth and Planetary Science Letters* 431, 127-139.

685

- Blake, W., Jr. 1977. Glacial sculpture along the east-central coast of Ellesmere Island,
- 687 Arctic Archipelago. Current Research, Part C, Geological Survey of Canada, Paper 77-
- 688 1C, 107-115.

689

- 690 Briner, J. P., Miller, G. H., Davis, P. T., Bierman, P. R., and Cafee, M., 2003. Last Glacial
- Maximum ice sheet dynamics in Arctic Canada inferred from young erratics perched
- on ancient tors. *Quaternary Science Reviews*, 22: 437-444.

693

- Brown, T.A., Belt, S.T., 2012. Closely linked sea ice-pelagic coupling in the Amundsen
- 695 Gulf revealed by the sea ice diatom biomarker IP25. Journal of plankton research 34,
- 696 647-654.

697

- Buch E. 2000a. A monograph on the physical oceanography of the Greenland waters.
- 699 Danish Meteorological Institute Scientific Report, 00-12.

700

- 701 Buch E. 2000b. Air-sea-ice conditions off southwest Greenland, 1981–1997. *Journal*
- 702 of Northwest Atlantic Fisheries Science 26, 1–14.

703

- Buizert, C., Gkinis, V., Severinghaus, J.P., He, F., Lecavalier, B.S., Kindler, P.,
- Leuenberger, M., Carlson, A.E., Vinther, B., Masson-Delmotte, V., White, I.W.C., Liu, Z.,
- 706 Otto-Bliesner, B., Brook, E.J., 2014. Greenland temperature response to climate
- forcing during the last deglaciation. Science 345, 1177-1180. DOI:
- 708 10.1126/science.1254961

709

- 710 Campbell, D C, de Vernal, A., 2009. CCGS Hudson Expedition 2008029: marine
- 711 geology and paleoceanography of Baffin Bay and adjacent areas, Nain, NL to Halifax,
- NS, August 28-September 23. Geological Survey of Canada, Open File 5989, 2009,
- 713 212 pages; 1 DVD, doi:10.4095/261330

714

- 715 Clark, P.U., Dyke, A.S., Shakun, D., Carlson, A.E., Clark, J., Wohlfarth, B., Mitrovica, J.X.,
- Hostetler, S.W., McCabe, A.M., 2009. The Last Glacial Maximum. Science 325, 710-
- 717 714.

718

- 719 Dahl-Jensen, D. and al., e., 1998: Past Temperatures Directly from the Greenland Ice
- 720 Sheet. *Science*, 282: 268-271.

- Darling, K. F., Kucera, M., Kroon, D., Wade, C.M., 2006. A resolution for the coiling
- 723 direction paradox in *Neogloboquadrina pachyderma*. *Paleoceanography* 21,
- 724 PA2011, doi:10.1029/2005PA001189.

- de Vernal, A., Bilodeau, G., Hillair -Marcel, C., Kassou, N., 1992. Quantitative
- assessment of carbonate dissolution in marine sediments from foraminifer linings
- vs. shell ratios: example from Davis Strait, NW North Atlantic, Geology, 20: 527-530.

729

- 730 Domack, E.W., Harris, P.T., 1998. A new depositional model for ice shelves, based
- upon sediment cores from the Ross Sea and the Mac. Roberson shelf, Antarctica.
- 732 *Annals of Glaciology* 27, 281-284.

733

- Dowdeswell, J.A., Hogan, K.A., Ó Cofaigh, C., Fugelli, E.M.G., Evans, J., Noormets, R.,
- 735 2014. Late Quaternary ice flow in aWest Greenland fjord and cross-shelf trough
- 736 system: submarine landforms from Rink Isbrae to Uummannaq shelf and slope.
- 737 *Quat. Sci. Rev.* 92, 292-309. <a href="http://dx.doi.org/10.1016/j.quascirev.2013.09.007">http://dx.doi.org/10.1016/j.quascirev.2013.09.007</a>.

738

- 739 Dyke, A. S., Andrews, J. T., Clark, P. U., England, J. H., Miller, G. H., Shaw, J., and
- 740 Veillette, J. J., 2002: The Laurentide and Innuitian ice sheets during the Last Glacial
- 741 Maximum. *Quaternary Science Reviews*, 21, 9-31.

742

- Eberl, D.D., 2003. User guide to RockJock: A program for determining quantitative
- 744 mineralogy from X-ray diffraction data. United States Geological Survey, Open File
- 745 Report 03-78, 40 pp, Washington, DC.

746

- 747 Eiríksson, J., Knudsen, K.L., Haflidason, H., Henriksen, P., 2000. Late-glacial and
- Holocene palaeoceanography of the North Icelandic shelf. Journal of Quaternary
- 749 *Science* 15, 23-42.

750

- 751 England, J. 1999. Coalescent Greenland and Innuitian ice during the Last Glacial
- 752 Maximum: Revising the Ouaternary of the Canadian High Arctic. *Ouaternary Science*
- 753 *Reviews* 18, 421–426, http://dx.doi.org/10.1016/S0277-3791(98)00070-5.

754

- England, J., Atkinson, N., Bednarski, J., Dyke, A.S., Hodgson, D.A., Ó Cofaigh, C. 2006.
- 756 The Innuitian Ice Sheet: configuration, dynamics and chronology. *Quaternary*
- 757 *Science Reviews* 25, 689-703.

758

- 759 Fahl, K., Stein, R., 2012. Modern seasonal variability and deglacial/Holocene change
- of central Arctic Ocean sea ice cover: New insights from biomarker proxy records.
- 761 Earth and Planetary Science Letters 351–352, 123–133.

762

- Grobe, H., 1987. A simple method for the determination of ice-rafted debris in
- sediment cores. *Polarforschung* 57 (3), 123-126.

- Hald, M., Korsun, S. 1997. Distribution of modern benthic foraminifera from fjords of
- 767 Svalbard, European Arctic. *Journal of Foraminiferal Research* 27, 101–122.

Hemming, S.R., 2004. Heinrich events: massive late Pleistocene detritus layers of the North Atlantic and their global climate imprint. *Rev. Geophys.* 42, RG1005.

Hesse, R., Khodabakhsh, S. 2016. Anatomy of Labrador Sea Heinrich layers. *Marine Geology* 380, 44-86. http://dx.doi.org/10.1016/j.margeo.2016.05.019

Hesse, R., Khodabakhsh, S., Klaucke, I., Ryan, WBF., 1997. Asymmetrical turbid surface-plume deposition near ice-outlets of the Pleistocene Laurentide ice sheet in the Labrador Sea. *Geo-Marine Letters*, 17, 179-187.

Hillaire-Marcel, C., de Vernal, A., 2008. Stable isotope clue to episodic sea-ice formation in the glacial North Atlantic. Earth and Planetary Science Letters, 268, 143-150.

Hillaire-Marcel, C., de Vernal, A., Aksu, A.E., Macko, S., 1989. High-resolution isotopicand micropaleontological studies of upper Pleistocene sediments at ODP Site 645, Baffin Bay, Proceedings of the Ocean Drilling Program, 105B: 599-616.

Hofmann, J.C., Knutz, P.C., Nielsen, T., Kuijpers, A., 2016. Seismic architecture and evolution of the Disko Bay trough-mouth fan, central West Greenland margin, *Quaternary Science Reviews*, http://dx.doi.org/10.1016/j.quascirev.2016.05.019

Holland, D.M., Thomas, R.H., de Young, B., Ribergaard, M.H., Lyberth, B., 2008.
 Acceleration of Jakobshavn Isbræ triggered by warm subsurface oceanwaters.
 Nature Geoscience 1 (10), 659e664. http://dx.doi.org/10.1038/ngeo316.

Hulbe, C.L., 1997. An ice shelf mechanism for Heinrich layer production, *Paleoceanography* 12, 711 –717.

Hulbe, C. L., MacAyeal, D. R., Denton, G. H., Kleman, J., and Lowell, T. V., 2004:
 Catastrophic ice shelf breakup as the source for Heinrich event icebergs.
 *Palaeoceanography*, 19: 1 of 15, doi.10.1029/2003:PA000890, 002004.

Jackson, R., Carlson, A.E., Hillaire-Marcel, C., Wacker, L., Vogt, C., Kucera, M., 2017. Asynchronous instability of the North American-Arctic and Greenland ice sheets during the last deglaciation. *Quaternary Science Reviews* 164, 140-153. http://dx.doi.org/10.1016/j.quascirev.2017.03.020.

Jennings, A.E., Andrews, J.T., Ó Cofaigh, C., St. Onge, G., Sheldon, C., Belt, S.T., Cabedo-Sanz, P., Hillaire-Marcel, C. 2017. Ocean forcing of Ice Sheet Retreat in Central West Greenland from LGM through Deglaciation. *Earth and Planetary Science Letters* 472, 1-13.

- 812 Jennings, A.E., Andrews, J.T., Wilson, L., 2011b. Holocene Environmental Evolution of
- the SE Greenland Shelf North and South of the Denmark Strait: Irminger and East
- Greenland Current Interactions. Quaternary Science Reviews 30: 980-998.

- Jennings, A.E., Hald, M., Smith, L.M., and Andrews, J.T., 2006. Freshwater forcing
- 817 from the Greenland Ice Sheet during the Younger Dryas: Evidence from
- southeastern Greenland shelf cores: *Quaternary Science Reviews* 25, 282–298,
- 819 doi:10.1016/j.quascirev.2005.04.006.

820

- Jennings, A.E., Helgadottir, G., 1994. Foraminiferal assemblages from the fjords and
- shelf of eastern Greenland. *J. Foraminifer. Res.* 24 (2), 123e144.
- 823 http://dx.doi.org/10.2113/gsjfr.24.2.123.

824

- Jennings, A.E., Sheldon, C., Cronin, T.M., Francus, F., Stoner, J., Andrews, J., 2011a. The
- 826 Holocene history of Nares Strait, transition from glacial bay to Arctic-Atlantic
- throughflow. *Oceanography* 24, no. 3, 26-41.

828

- Jennings, A. E., Tedesco, K. A., Andrews, J. T., and Kirby, M. E., 1996. Shelf erosion and
- 830 glacial ice proximity in the Labrador Sea during and after Heinrich events (H-3 or 4
- to H-0) as shown by foraminifera. *In* Andrews, J. T., Austin, W. E. N., Bergsten, H., and
- 832 Jennings, A. E. (eds.), *Late Quaternary Palaeoceanography of the North Atlantic*
- 833 *Margins*: Geological Society Special Publications, 29-49.

834

- Iennings, A.E., Walton, M.E., Cofaigh, C.O., Kilfeather, A., Andrews, J.T., Ortiz, J.D., et
- al., 2014. Paleoenvironments during Younger Dryas-early Holocene retreat of the
- 837 Greenland ice sheet from outer Disko Trough, central west Greenland. *J. Quat. Sci.* 29
- 838 (1), 27**e**40. <a href="http://dx.doi.org/10.1002/jqs.2652">http://dx.doi.org/10.1002/jqs.2652</a>.

839

- Kaufman, D.S., Williams, K.M. (compilers), 1992. Radiocarbon Date List VII: Baffin
- Island, N.W.T., Canada. INSTAAR Occasional Paper 48. Institute of Arctic and Alpine
- 842 Research, University of Colorado, Boulder.

843

- Knutz, P. C., M.-A. Sicre, H. Ebbesen, S. Christiansen, and A. Kuijpers, 2011. Multiple-
- stage deglacial retreat of the southern Greenland Ice Sheet linked with Irminger
- 846 Current warm water transport, *Paleoceanography* 26, PA3204,
- 847 doi:10.1029/2010PA002053.

848

- Li, G., Piper, D. J. W., and Campbell, D. C., 2011: The Quaternary Lancaster Sound
- trough-mouth fan, NW Baffin Bay. *Journal of Quaternary Science*, 26: 511-522.
- Lloyd, J. M. 2006. Modern distribution of benthic foraminifera from Disko Bugt, West
- 852 Greenland. Journal of Foraminiferal Research 36, 315–331.

853

- Lloyd, J.M., Moros, M., Perner, K., Telford, R.J., Kuijpers, A., Jansen, E., et al., 2011.A
- 855 100 yr record of ocean temperature control on the stability of JakobshavnIsbrae,
- 856 West Greenland. *Geology* 39 (9), 867-870. http://dx.doi.org/10.1130/G32076.1.

- Löwemark, L., O'Regan, M., Hanebuth, T.J.J., Jakobsson, M., 2012. Late Quaternary
- spatial and temporal variability in Arctic deep-sea bioturbation and its relation to
- 860 Mn cycles. *Palaeogeography, Palaeoclimatology, Palaeoecology* 365-366, 192-208.

- Lucci, RG and Rebesco, M., 2007. Glacial contourites on the Antarctic Peninsula
- margin: insight for palaeoenvironmental and palaeoclimatic conditions. Geological
- 864 Society, London, Special Publications, 276: 111-127.

865

Marcott et al., 2011. Ice-shelf collapse from subsurface warming as a trigger for Heinrich Events. PNAS 108. No. 33 p. 13415-13419

868

- 869 McManus, J.F., Francois, R., Gherardi, J.-M., Keigwin, L.D., Brown-Leger, S., 2004.
- 870 Collapse and rapid resumption of the Atlantic meridional circulation linked to
- deglacial climate change. Nature 428, 834-837.

872

- 873 Münchow A., Falkner, A. Melling, H., 2015. Baffin Island and West Greenland Current
- 874 Systems in northern Baffin Bay. *Progress in Oceanography* 132, 305–317

875

- 876 Ó Cofaigh C., Andrews JT, Jennings AE, Dowdeswell JA, Hogan KA, Kilfeather AA, et
- al. (2013a) Glacimarine lithofacies, provenance and depositional processes on a West
- 678 Greenland trough-mouth fan. Journal of Quaternary Science 28. Available at:
- 879 http://dx.doi.org/10.1002/jqs.2569: doi:10.1002/jqs.2569.

880

- 6 O Cofaigh C, Dowdeswell J.A., 2001. Laminated sediments in glacimarine environments:
- diagnostic criteria for their interpretation. *Quaternary Science Reviews* 20, 1411-1436.

883

- Ó Cofaigh C., Dowdeswell J.A., Jennings A.E., Hogan K.A., Kilfeather A., Hiemstra
- J.F., et al. (2013b) An extensive and dynamic ice sheet on the West Greenland shelf
- during the last glacial cycle. *Geology* 41(2): 219–222: doi:10.1130/G33759.1.

887

- Nørgaard-Pedersen, N., Spielhagen, R.F., Erlenkeuser, H., Grootes, P.M., Heinemeier,
- 889 J., Knies, J., 2003. Arctic Ocean during the Last Glacial Maximum: Atlantic and polar
- domains of surface water mass distribution and ice cover. Paleoceanography 18,
- 891 doi:10.1029/2002PA000781, 2003.

892

- 893 Perner, K., Moros, M., Jennings, A., Lloyd, J.M., Knudsen, K.L., 2012. Holocene
- palaeoceanographic evolution off West Greenland. *The Holocene* 23, 374-387.

895

- 896 Piénkowski, A.J., England, J.H., Furze, M.F.A., Marret, F., Eynaud, F., Vilks, G., Maclean,
- 897 B., Blasco, S., Scourse, J.D., 2012. The deglacial to postglacial marine environments of
- 898 SEBarrow Strait, Canadian Arctic Archipelago. *Boreas* 41 (2), 141-179.
- 899 http://dx.doi.org/10.1111/j.1502-3885.2011.00227.x.

- 901 Polyak, L., Korsun, S., Febo, L.A., Stanovoy, V., Khusid, T., Hald, M., Paulsen, B.E.,
- 902 Lubinski, D.J., 2002. Benthic foraminiferal assemblages from the southern Kara Sea,

- a river influenced Arctic marine environment. *Journal Foraminiferal Research* 32,
- 904 252–273.
- 905
- 906 Post, A.L., Galton-Fenzi, B.K., Riddle, M.J., Herraiz-Borreguero, L., O'Brien, P.E.,
- 907 Hemer, M.A., McMinn, A., Rasch, D., Craven, M., 2014. Modern sedimentation,
- 908 circulation and life beneath the Amery Ice Shelf, East Antarctica. *Continental Shelf*
- 909 Research 74. 77-87.
- 910
- 911 Quillmann, U., Andrews, J. T., and Jennings, A. E., 2009: *Radiocarbon Date List XI:*
- 912 East Greenland shelf, West Greenland Shelf, Labrador Sea. Baffin Island shelf, Baffin
- 913 Bay, Nares Strait, and Southwest to Northwest Icelandic shelf. Occasional Paper No.
- 59, INSTAAR, University of Colorado, Boulder, Boulder.

- Ramsey, C.B. and Lee, S., 2013. Recent and planned developments of the program
- 917 OxCal. Radiocarbon 55, 720-730.

918

- Reeh, N., Thomsen, H. H., Higgins, A. K., and Weidick, A., 2001: Sea ice and the
- 920 stability of north and northeast Greenland floating glaciers. *In* Jeffries, M. O. and
- 921 Eicken, H. (eds.), *Annals of Glaciology, Vol 33*, 474-480.

922

- Reimer, P.J., Bard, E., Bayliss, A., Beck, J.W., Blackwell, P.G., Ramsey, C.B., Grootes,
- 924 P.M., Guilderson, T.P., Haflidason, H., Hajdas, I., Hatté, C., Heaton, T.J., Hoffmann,
- 925 D.L., Hogg, A.G., Hughen, K.A., Kaiser, K.F., Kromer, B., Manning, S.W., Niu, M.,
- Reimer, R.W., Richards, D.A., Scott, E.M., Southon, J.R., Staff, R.A., Turney, C.S.M.,
- van der Plicht, J., 2013. IntCal13 and Marine13 radiocarbon age calibration curves 0-
- 928 50,000 years cal BP. Radiocarbon 55, 1869–1887. http://dx.doi.org/10.2458/azu\_js\_rc.
- 929 55.16947.

930

- Reineck, H.E., Singh, I.B., 1980. Depositional Sedimentary Environments. Springer-
- 932 Verlag, NY.

933

- 934 Sarnthein, M., et al., Variations in Atlantic surface ocean paleoceanography, 50 –80 N:
- A time-slice record of the last 30,000 years, Paleoceanography, 10(6), 1063–1094, 1995.
- 936 Schafer, C.T., Cole, F.E., 1988. Environmental associations of Baffin Island fjord
- 937 agglutinated foraminifera. Abh. Geol. Bundesanst, 307.

938

- 939 Seidenkrantz, M.-S., 2013. Benthic foraminifera as palaeo sea-ice indicators in the
- 940 subarctic realm-examples from the Labrador Sea-Baffin Bay region. *Quaternary Science*
- 941 Reviews 79, 135-144. http://dx.doi.org/10.1016/j.quascirev.2013.03.014

942

- 943 Shaffer, G., Olsen, S.M., Bjerrum, C.J., 2004. Ocean subsurface warming as a
- mechanism for coupling Dansgaard-Oeschger climate cycles and ice-rafting events.
- 945 Geophysical Research Letters 31, L24202. doi:10.1029/2004GL020968.

- 947 Sheldon, C., Jennings, A., Andrews, J.T., Ó Cofaigh, C., Hogan, K., Dowdeswell, J.A.,
- 948 Seidenkrantz, M-S., 2016. Ice stream retreat following the LGM and onset of the west

- 949 Greenland current in Uummannaq Trough, west Greenland. Quaternary Science Reviews,
- 950 http://dx.doi.org/10.1016/j.quascirev.2016.01.019

- 952 Simon, Q., Hillaire-Marcel, C., St-Onge, G., Andrews, J.T., 2014. Northeastern
- 953 Laurentide, western Greenland and southern Innuitian ice stream dynamics during the last
- 954 glacial cycle. Journal of Quaternary Science 29(1): 14-26. DOI: 10.1002/jqs.2648

955

- 956 Simon Q, St-Onge G, Hillaire-Marcel C., 2012. Late Quaternary chronostratigraphic
- 957 framework of deep Baffin Bay glaciomarine sediments from high-resolution
- paleomagnetic data. Geochemistry, Geophysics, Geosystems 13: Q0AO03. doi: 10.1029/
- 959 2012GC004272

960

- 961 Simon, Q., Thouveny, N., Bourles, D.L., Nuttin, L., Hillaire-Marcel, C., St-Onge, G.,
- 2016. Authigenic <sup>10</sup>Be/ <sup>9</sup>Be ratios and <sup>10</sup>Be-fluxes (<sup>230</sup>Th<sub>xs</sub>-normalized) in central Baffin
- 963 Bay sediments during the last glacial cycle: Paleoenvironmental implications. *Quaternary*
- 964 Science Reviews 140, 142-162.

965

- Slabon, P., Dorschel, B., Jokat, W., Myklebust, R., Hebbeln, D., Gebhardt, C., 2016.
- Greenland ice sheet retreat history in the northeast Baffin Bay based on high-resolution
- bathymetry. Quaternary Science Reviews 154, 182-198.
- 969 <u>http://dx.doi.org/10.1016/j.quascirev.2016.10.022</u>

970

- 971 Slubowska, M.A., Koç, N., Rasmussen, T.L., Klitgaard-Kristensen, D., 2005. Changes in
- 972 the flow of Atlantic water into the Arctic Ocean since the last deglaciation: evidence from
- 973 the northern Svalbard continental margin, 80 N. Paleoceanography 20, PA4014.
- 974 doi:10.1029/2005PA001141.

975

- 976 Stern, J.V., Lisiecki, L.E. 2013. North Atlantic circulation and reservoir age changes over
- 977 the past 41,000 years. Geophysical Research Letters 40: 3693-3697.
- 978 doi:10.1002/grl.50679, 2013.

979

- 980 Straneo, F., Sutherland, D.A., Holland, D., Gladish, C., Hamilton, G.S., Johnson, H.L.,
- Rignot, E., Xu, Y., Koppes, M., 2012. Characteristics of ocean waters reaching
- 982 Greenland's glaciers. *Annals of Glaciology* 53(60), 202-210.
- 983 doi:10.3189/2012AoG60A059

984

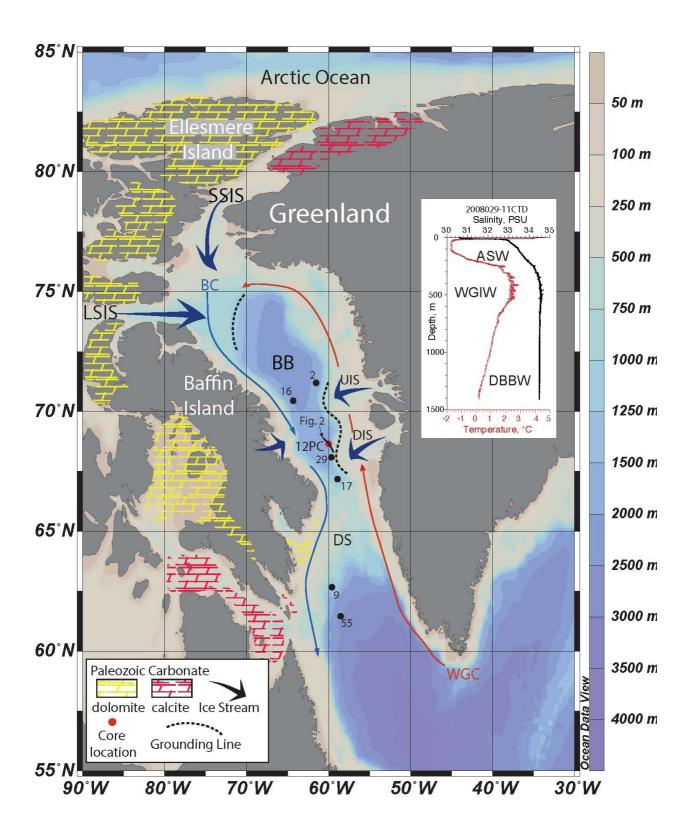
- Tang, C.C.L., Ross, C.K., Yao, T., Petrie, B., DeTracey, B.M., Dunlap, E., 2004. The
- 986 circulation, water masses and sea-ice of Baffin Bay. Progress in Oceanography 63, 183-
- 987 228.

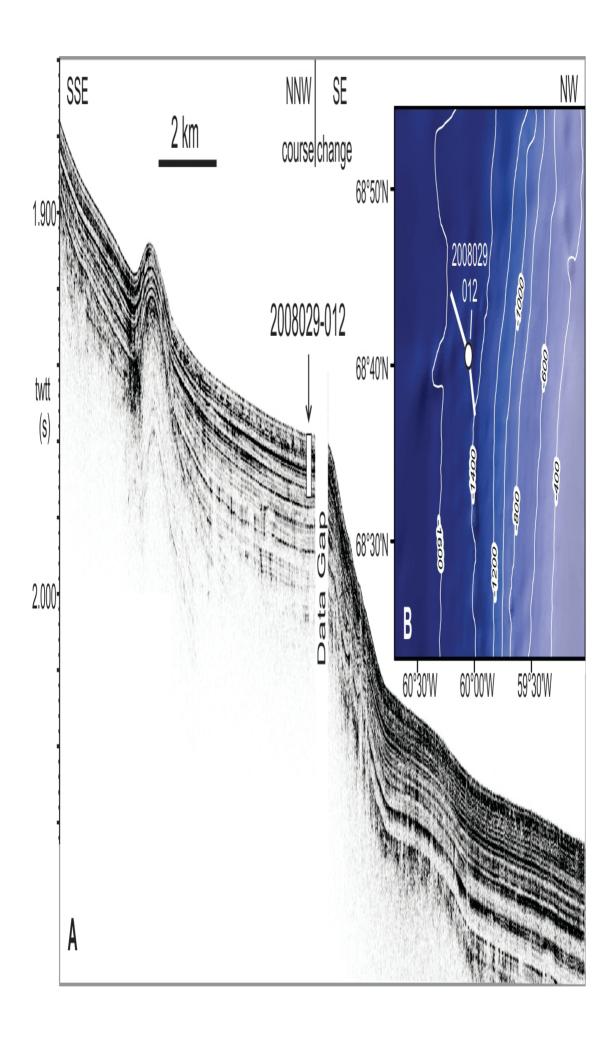
988

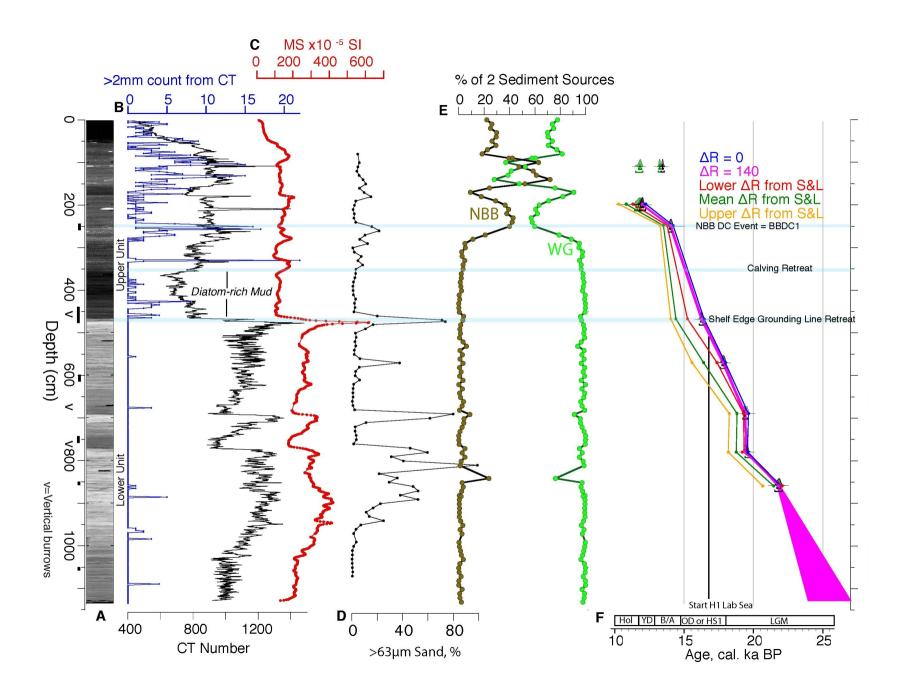
- Wetzel, A., 1991. Ecologic interpretation of deep-sea trace fossil co=unities.
- Palaeogeography, Palaeoclimatology, Palaeoecology 85, 47-69.

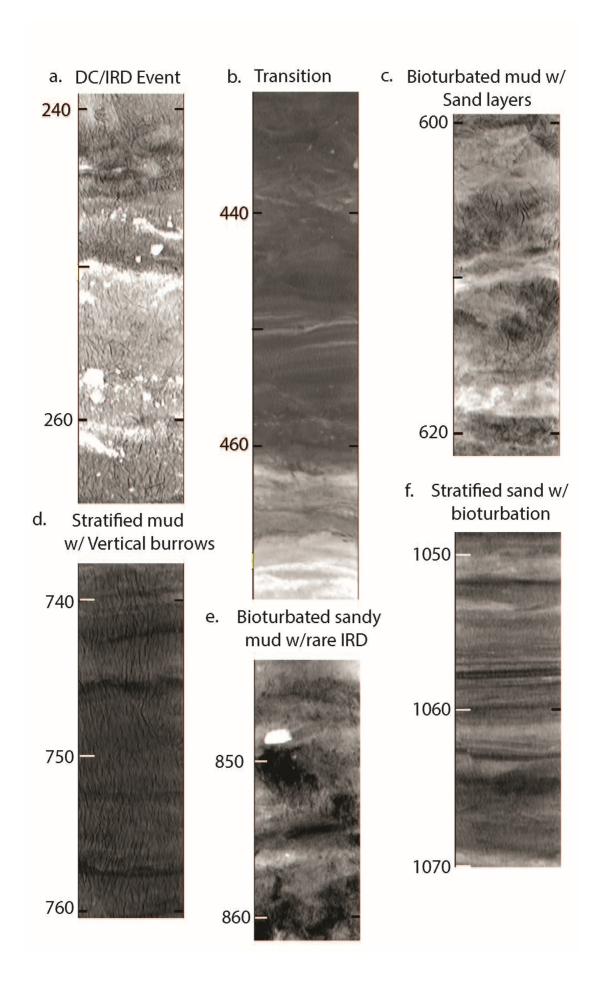
- Wollenburg, J.E., Knies, J., Mackensen, A., 2004. High-resolution paleoproductivity
- 993 fluctuations during the past 24 kyr as indicated by benthic foraminifera in the

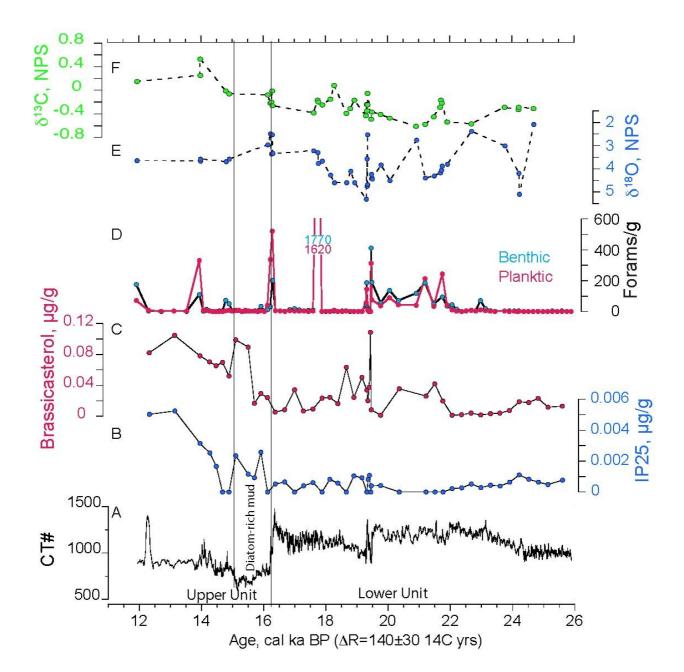
994 marginal Arctic Ocean. Palaeogeography, Palaeoclimatology, Palaeoecology 204, 209-995 238. 996 Xiao, X., Fahl, K., Stein, R., 2013. Biomarker distributions in surface sediments from the 997 998 Kara and Laptev seas (Arctic Ocean): indicators for organic-carbon sources and sea ice 999 coverage. Quaternary Science Reviews 79, 40-52. 1000 Zreda, M., J. England, F. Phillips, D. Elmore, and P. Sharma. 1999. Unblocking of the 1001 1002 Nares Strait by Greenland and Ellesmere Ice-Sheet retreat 10,000 years ago. Nature 1003 398,139–142, http://dx.doi.org/10.1038/18197 1004



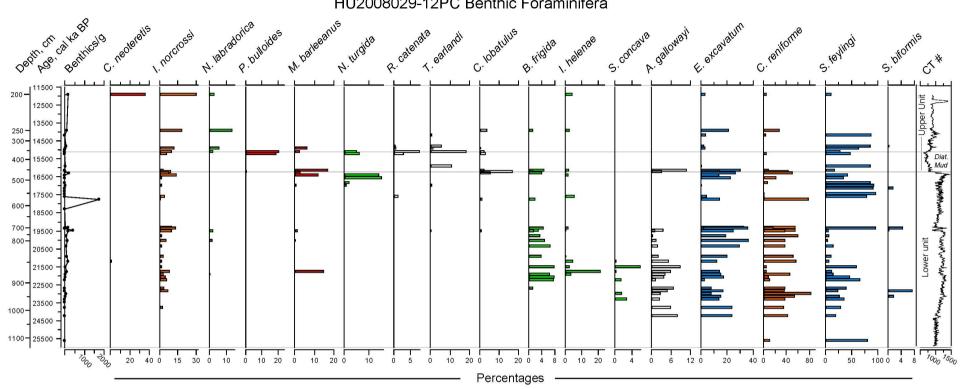








## HU2008029-12PC Benthic Foraminifera



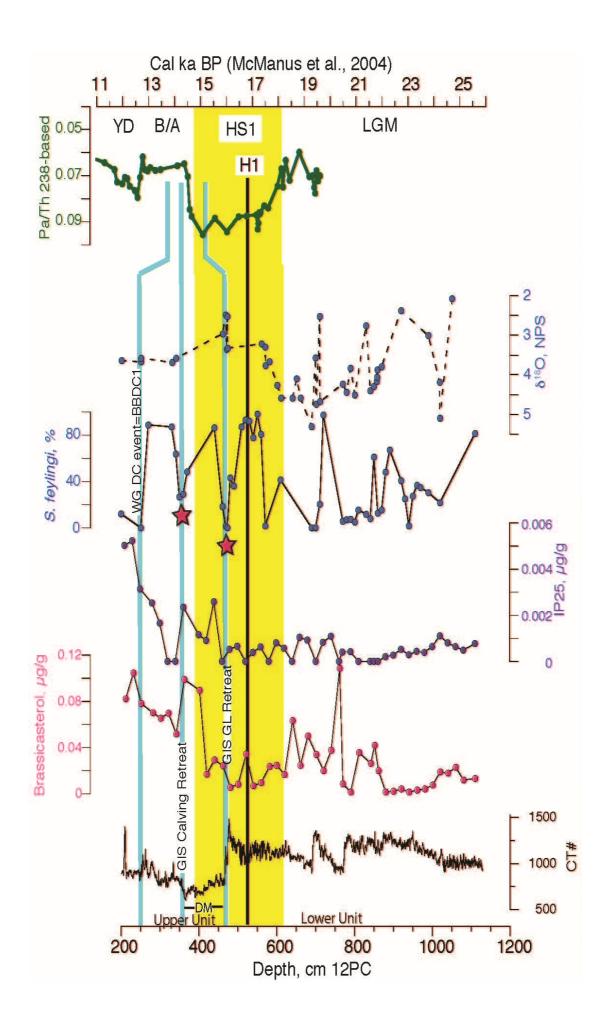


Table 1. Radiocarbon ages and their calibrations with varying  $\Delta R$ .

## HU2008029-12PC

1102000023 12	10			
Date	Depth 1	.4C e1	ror	ΔR Date (14C age
CURL14065	201. 5	10760	35	0 CURL14065 wi
CURL14065	201. 5	10760	35	140 CURL14065 wi
CURL14065	201. 5	10760	35	470 CURL14065 wi
CURL14065	201. 5	10760	35	900 CURL14065 wi
CURL14065	201. 5	10760	35	1340 CURL14065 wi
AA90386	251.5	12666	61	0 AA90386 with
AA90386	251. 5	12666	61	140 AA90386 with
AA90386	251. 5	12666	61	380 AA90386 with
AA90386	251. 5	12666	61	630 AA90386 with
AA90386	251.5	12666	61	900 AA90386 with
CURL16671	469. 5	14030	40	0 CURL16671 wi
CURL16671	469. 5	14030	40	140 CURL16671 wi
CURL16671	469.5	14030	40	850 CURL16671 wi
CURL16671	469.5	14030	40	1260 CURL16671 wi
CURL16671	469.5	14030	40	1500 CURL16671 wi
CURL18165	571.5	15150	60	0 CURL18165 wi
CURL18165	571.5	15150	60	140 CURL18165 wi
CURL18165	571.5	15150	60	500 CURL18165 wi
CURL18165	571.5	15150	60	1150 CURL18165 wi
CURL18165	571.5	15150	60	1750 CURL18165 wi
CURL14067	690. 5	16660	45	0 CURL14067 wi
CURL14067	690. 5	16660	45	140 CURL14067 wi
CURL14067	690. 5	16660	45	290 CURL14067 wi
CURL14067	690. 5	16660	45	720 CURL14067 wi
CURL14067	690. 5	16660	45	1250 CURL14067 wi
CURL16663	780. 5	16600	50	0 CURL16663 wi
CURL16663	780. 5	16600	50	140 CURL16663 wi
CURL16663	780. 5	16600	50	290 CURL16663 wi
CURL16663	780. 5	16600	50	720 CURL16663 wi
CURL16663	780. 5	16600	50	1250 CURL16663 wi
CURL18628	859. 5	18540	80	0 CURL18628 wi
CURL18628	859.5	18540	80	140 CURL18628 wi
CURL18628	859.5	18540	80	-50 CURL18628 wi
CURL18628	859.5	18540	80	420 CURL18628 wi
CURL18628	859. 5	18540	80	1010 CURL18628 wi

HU87033-009 LCF,	500-501 cm;	Jennings et al.,	1996	
AA-9364		14980	90	0 AA-9364 with
AA-9364		14980	90	140 AA-9364 with
AA-9364		14980	90	500 AA-9364 with

AA-9364	1	4980 9	0 1150 AA-9364	with
AA-9364	1-	4980 9	0 1750 AA-9364	with
HU75009-IV-055PC,	115-117 cm; Kaufma	n and Williams, 1	1992	
AA-5999	1.	5010 10	5 0 AA-5999	with
AA-5999	1.	5010 10	5 140 AA-5999	with
AA-5999	1.	5010 10	5 500 AA-5999	with
AA-5999	1.	5010 10	5 1150 AA-5999	with
AA-5999	1	5010 10	5 1750 AA-5999	with

	C 1			0 :	C	Caliba					
sigma_	from 1 12306	.s1gma	12075	2sigma	12430	2sigma	12028	mean	12215	error	109
	12026		11865		12100		11755		11937		86
	11317		11210		11432		11161		11282		70
	10868		10706		10972		10667		10805		79
	10291		10196		10372		10176		10260		51
	14279		14051		14542		13964		14208		142
	14095		13926		14165		13840		14007		83
	13845		13665		13930		13555		13748		91
	13552		13392		13657		13332		13484		81
	13312		13180		13375		13114		13246		66
	16511		16309		16632		16233		16423		102
	16311		16144		16424		16045		16232		90
	15282		15148		15375		15076		15221		73
	14507		14193		14701		14136		14398		155
	14086		13947		14143		13873		14011		68
	18035		17854		18130		17740		17941		94
	17887		17687		17973		17598		17785		97
	17465		17236		17549		17125		17345		110
	16491		16261		16631		16174		16390		117
	15680		15408		15776		15297		15541		128
	19698		19528		19832		19467		19631		91
	19550		19372		19609		19260		19449		88
	19368		19168		19466		19070		19268		99
	18850		18739		18905		18674		18791		57
	18328		18149		18395		18039		18226		90
	19634		19467		19749		19360		19553		91
	19480		19283		19560		19203		19380		93
	19257		19061		19385		18986		19177		99
	18802		18680		18856		18605		18735		62
	18267		18071		18337		17973		18160		94
	22113		21850		22271		21751		21993		131
	21916		21670		22057		21537		21795		127
	22175		21905		22301		21820		22051		128
	21594		21299		21746		21137		21442		149
	20772		20537	,	20913		20434		20662		119
						,		,			
	17878		17633		17984		17515		17752		120
	17725		17460		17883		17333		17599		136
	17281		16963		17437		16789		17115		161

16288 15443	16021 15143	16449 15656	15861 15041	16155 15318	140 155
17916	17650	18037	17513	17780	133
17785	17490	17925	17345	17634	147
17345	17000	17495	16800	17156	174
16345	16032	16538	15875	16200	163
15528	15180	15733	15060	15367	174

12207 11943 11270 10796 10250 14180 14009 13751 13478 13246 16416 16230 15218 14378 14014 17943 17786 17349 16381 15544 19621 19455 19264 18793 18234 19551 19382 19173 18738 18163 21985 21798 22048 21444 20657	median	
11270 10796 10250 14180 14009 13751 13478 13246 16416 16230 15218 14378 14014 17943 17786 17349 16381 15544 19621 19455 19264 18793 18234 19551 19382 19173 18738 18163 21798 22048 21444		12207
10796 10250 14180 14009 13751 13478 13246 16416 16230 15218 14378 14014 17943 17786 17349 16381 15544 19621 19455 19264 18793 18234 19551 19382 19173 18738 18163 21985 21798 22048 21444		11943
10250 14180 14009 13751 13478 13246 16416 16230 15218 14378 14014 17943 17786 17349 16381 15544 19621 19455 19264 18793 18234 19551 19382 19173 18738 18163 21985 21798 22048 21444		11270
14180 14009 13751 13478 13246 16416 16230 15218 14378 14014 17943 17786 17349 16381 15544 19621 19455 19264 18793 18234 19551 19382 19173 18738 18163 21985 21798 22048 21444		10796
14009 13751 13478 13246 16416 16230 15218 14378 14014 17943 17786 17349 16381 15544 19621 19455 19264 18793 18234 19551 19382 19173 18738 18163 21985 21798 22048 21444		10250
13751 13478 13246 16416 16230 15218 14378 14014 17943 17786 17349 16381 15544 19621 19455 19264 18793 18234 19551 19382 19173 18738 18163 21985 21798 22048 21444		14180
13478 13246 16416 16230 15218 14378 14014 17943 17786 17349 16381 15544 19621 19455 19264 18793 18234 19551 19382 19173 18738 18163 21985 21798 22048 21444		14009
13246 16416 16230 15218 14378 14014 17943 17786 17349 16381 15544 19621 19455 19264 18793 18234 19551 19382 19173 18738 18163 21985 21798 22048 21444		13751
16416 16230 15218 14378 14014 17943 17786 17349 16381 15544 19621 19455 19264 18793 18234 19551 19382 19173 18738 18163 21985 21798 22048 21444		13478
16230 15218 14378 14014 17943 17786 17349 16381 15544 19621 19455 19264 18793 18234 19551 19382 19173 18738 18163 21985 21798 22048 21444		13246
15218 14378 14014 17943 17786 17349 16381 15544 19621 19455 19264 18793 18234 19551 19382 19173 18738 18163 21985 21798 22048 21444		16416
14378 14014 17943 17786 17349 16381 15544 19621 19455 19264 18793 18234 19551 19382 19173 18738 18163 21985 21798 22048 21444		16230
14014 17943 17786 17349 16381 15544 19621 19455 19264 18793 18234 19551 19382 19173 18738 18163 21985 21798 22048 21444		15218
17943 17786 17349 16381 15544 19621 19455 19264 18793 18234 19551 19382 19173 18738 18163 21985 21798 22048 21444		14378
17786 17349 16381 15544 19621 19455 19264 18793 18234 19551 19382 19173 18738 18163 21985 21798 22048 21444		14014
17349 16381 15544 19621 19455 19264 18793 18234 19551 19382 19173 18738 18163 21985 21798 22048 21444		17943
16381 15544 19621 19455 19264 18793 18234 19551 19382 19173 18738 18163 21985 21798 22048 21444		17786
15544 19621 19455 19264 18793 18234 19551 19382 19173 18738 18163 21985 21798 22048 21444		17349
19621 19455 19264 18793 18234 19551 19382 19173 18738 18163 21985 21798 22048 21444		16381
19455 19264 18793 18234 19551 19382 19173 18738 18163 21985 21798 22048 21444		
19264 18793 18234 19551 19382 19173 18738 18163 21985 21798 22048 21444		
18793 18234 19551 19382 19173 18738 18163 21985 21798 22048 21444		
18234 19551 19382 19173 18738 18163 21985 21798 22048 21444		
19551 19382 19173 18738 18163 21985 21798 22048 21444		
19382 19173 18738 18163 21985 21798 22048 21444		
19173 18738 18163 21985 21798 22048 21444		
18738 18163 21985 21798 22048 21444		
18163 21985 21798 22048 21444		
21985 21798 22048 21444		
21798 22048 21444		
22048 21444		
21444		
20657		
		20657

16154	
15302	
17781	
17633	
17159	
16195	
15356	